

Okinawa Institute of Science and Technology

Graduate University

Thesis submitted for the degree

Doctor of Philosophy

**Role of 5' - 3' exoribonuclease Xrn1 in
energy expenditure and control of obesity**

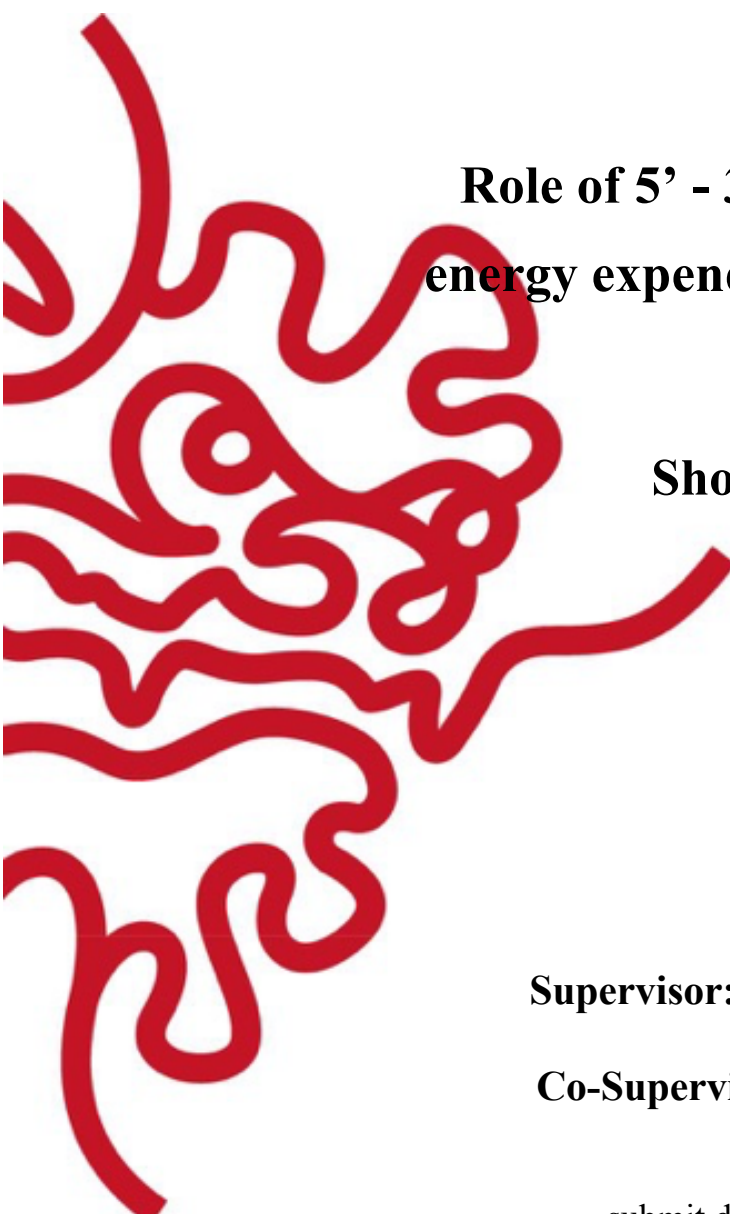
by

Shohei Takaoka

Supervisor: Tadashi Yamamoto

Co-Supervisor: Hiroaki Kitano

submit date (March 2020)



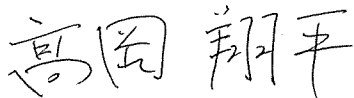
Declaration of Original and Sole Authorship

I, Shohei Takaoka, declare that this thesis entitled “Role of 5’ - 3’ exoribonuclease Xrn1 in energy expenditure and control of obesity” and the data presented in it are original and my own work.

I confirm that:

- This work was done solely while a candidate for the research degree at the Okinawa Institute of Science and Technology Graduate University, Japan.
- No part of this work has previously been submitted for a degree at this or any other university.
- References to the work of others have been clearly attributed. Quotations from the work of others have been clearly indicated, and attributed to them.
- In cases where others have contributed to part of this work, such contribution has been clearly acknowledged and distinguished from my own work.
- None of this work has been previously published elsewhere, with the exception of the following: (provide list of publications or presentations, or delete this part).
(If the work of any co-authors appears in this thesis, authorization such as a release or signed waiver from all affected co-authors must be obtained prior to publishing the thesis. If so, attach copies of this authorization to your initial and final submitted versions, as a separate document for retention by the Graduate School, and indicate on this page that such authorization has been obtained).

Signature:



Date:

2020.03.22

Abstract

Gene expression of eukaryotes is regulated by various processes including mRNA degradation. Dysregulation of mRNA degradation is now considered to be a possible cause of various disease including cancer, neurodegenerative disease, diabetes, and obesity. 5' - 3' exoribonuclease Xrn1 functions at the last step of mRNA degradation. Recent studies showed that Xrn1 forms specific cytoplasmic messenger ribonucleoprotein (mRNP) granules in post-synapse to regulate local translation. However, there are no physiological studies that have investigated the function of Xrn1 in the brain. Therefore, I generated forebrain specific Xrn1 knockout mice for the first time and analyzed their phenotype. Interestingly, the knockout mice showed obesity and hyperphagia. Energy homeostasis is regulated by various organs including central nervous systems and peripheral metabolic tissues such as liver, pancreas, and adipose tissues, thus the development of obesity is often caused by the dysregulation of inter-organ communication. In response to metabolic cues, peripheral tissues produce hormones such as insulin and leptin. The hypothalamus sense changes in circulating blood glucose, insulin, and leptin and integrate those cues to maintain metabolic homeostasis. Blood analysis showed that the conditional Xrn1 knockout mice were hyperglycemic, hyperleptinemic, and hyperinsulinemic. Consistent with the above phenotype, I observed dysregulated expression of appetite and energy homeostasis related genes in the hypothalamus of the knockout mice. These data suggest that Xrn1 is required for the regulation of appetite and energy homeostasis related gene expression in the hypothalamus, and thus Xrn1 plays a role in energy expenditure and control of obesity.

Acknowledgements

I acknowledge following persons for their suggestion and comments in preparation of this thesis.

Prof. Tadashi Yamamoto: Supervisor, and helpful comments, providing resources to conduct all experiments, giving me greater freedom in conducting my thesis study, and suggestion in executing the experiments.

Prof. Hiroaki Kitano: Co-supervisor, and his valuable advices and helpful suggestions on how to proceed with my thesis.

Dr. Yasuhide Furuta and Dr. Takaya Abe: Collaborator who produced and provided me *Xrn1*^{flox/+} mice.

Dr. Akinori Takahashi: Post doc, who provided the proper guidance and experimental expertise in helping me design the project, teaching me experimental techniques and their analysis, as well as for interpreting the data.

Dr. Patrick Stoney: Post doc, who provided guidance and expertise in metabolic regulation in the brain, as well as for teaching me how to do immunohistochemistry.

Dr. Haytham Mohamed Aly Mohamed: He kindly collected and analyzed metabolic data for me.

I also thank all the members of Yamamoto Unit, who provided important advice and suggestions.

Abbreviations

AgRP	agouti-related protein
α -MSH	α -melanocyte stimulating hormone
ARC	arcuate nucleus of hypothalamus
BKO	forebrain specific conditional knockout
CCR4	Carbon catabolite repression 4
DMH	dorsomedial nucleus of hypothalamus
GABA	gamma-Aminobutyric acid
JAK	Janus kinase
ME	median eminence
mRNA	messenger RNA
mRNPs	messenger ribonucleoprotein particles
mTOR	Mammalian target of rapamycin
NOT	negative on TATA-less
NPY	neuropeptide Y
P-bodies	Processing bodies
PABP	poly(A) binding protein
PI3K	Phosphoinositide 3-kinase
POMC	proopiomelanocortin
PVH	paraventricular nucleus of the hypothalamic
RER	respiratory exchange ratio
STAT	signal transducers and activators of transcription
VMH	ventromedial hypothalamic nucleus
XRN1	Exoribonuclease 1

List of Figures and tables

Figures

Figure 1.1| The two major mRNA decay pathways in eukaryotes.

Figure 1.2| Proposed diagram of Xrn1-dependent feedback regulation via indirect activation of transcription repressor.

Figure 1.3| Proposed diagram of Xrn1-dependent feedback regulation and nucleocytoplasmic shuttling of mRNA decay factors.

Figure 1.4| Xrn1 mediated mRNA decay-transcription feedback models proposed by three different groups.

Figure 1.5| Comparison of different mRNA silencing foci at post synapse under various stimuli.

Figure 3.1| Xrn1 knockout mice were embryonic lethal.

Figure 3.2| *Xrn1* knockout embryos express truncated protein.

Figure 3.3| Forebrain specific Xrn1 knockout mice were obese.

Figure 3.4| Appearance of Xrn1 knockout mice.

Figure 3.5| *Xrn1-BKO* mice exhibited hyperphagia.

Figure 3.6| *Xrn1-BKO* mice exhibited adiposity, and liver steatosis.

Figure 3.7| Expression of Xrn1 protein in mouse brain and peripheral tissues.

Figure 3.8| *Xrn1-BKO* mice exhibited hyperglycemia, hyperleptinemia, and hyperinsulinemia.

Figure 3.9| Xrn1-BKO mice displayed increased VCO₂, energy expenditure, and constant RER.

Figure 3.10| *Xrn1-BKO* mice didn't show statistical changes in activity.

Figure 3.11| *Xrn1-BKO* mice exhibited upregulation of appetite and energy homeostasis related genes in hypothalamus.

Figure 3.12| Leptin and insulin signaling related protein expression in *Xrn1-BKO* mice hypothalamus.

Figure 3.13| *Xrn1-BKO* mice displayed increased AgRP expression and decreased Pomc expression in hypothalamus.

Figure 3.14| Volcano plot from the proteomics analysis in hypothalamus.

Figure 3.15| Validation of mass spec result by qPCR and immunoblotting.

Tables

Table 2.1| gRNA and ssODN used for Xrn1 mice generation.

Table 2.2| Primer sets used for genotyping.

Table 2.3| Primer sets used for qPCR.

Table 3.1| Differentially expressed proteins related to metabolism and hormone signal.

Table 3.2| Differentially expressed proteins related to brain.

Table 3.3| Differentially expressed proteins related to mRNA metabolism.

Table of contents

Chapter 1 Introduction	1
1.1 Introduction to mRNA degradation in eukaryotes	2
1.2 Feedback regulation between mRNA degradation and transcription via Xrn1	6
1.3 mRNP granules and local translation regulation	19
1.4 Role of mRNA degradation in physiology.....	23
1.5 Aim of the study.....	25
Chapter 2 Material and methods	26
2.1 Mice	26
2.2 Genotyping.....	27
2.3 Daily food intake analysis.....	28
2.4 Blood analysis.....	29
2.5 Metabolic analysis	29
2.6 Immunoblotting.....	30
2.7 Antibodies for immunoblotting.....	31
2.8 Quantitative real-time RT-PCR (qRT-PCR).....	32
2.9 Proteomics analysis.....	34
2.10 Immunohistochemistry	35
2.11 Primers	37
Chapter 3 Results	39
3.1 Xrn1 whole-body knockout causes embryonic lethality.....	39
3.2 Forebrain specific Xrn1 knockout mice were obese	43
3.3 Xrn1-BKO mice exhibited hyperphagia, adiposity, and liver steatosis	43

3.4 Xrn1-BKO mice exhibited hyperglycemia, hyperleptinemia, and hyperinsulinemia ..	49
3.5 Metabolic alteration in Xrn1-BKO mice	49
3.6 Xrn1-BKO mice exhibited upregulation of appetite and energy homeostasis related genes in hypothalamus	53
3.7 Proteomics analysis in Xrn1-BKO hypothalamus	58
Chapter 4 Discussion	63
4.1 Function of Xrn1 in embryo genesis	63
4.2 Xrn1 controls energy homeostasis in hypothalamus	64
Chapter 5 Reference.....	69

Chapter 1 Introduction

Eukaryotic gene expression begins with transcription. Transcribed messenger RNA (mRNA) is processed in the nucleus to become mature mRNA. Mature mRNA is transported from the nucleus to the cytoplasm where it is used as a template for translation. After translation, all mRNAs are eventually degraded. Initially, many studies focused on transcription. However, it is now clear that transcription is just one step in the process of gene expression. In the past few decades, many enzymes involved in mRNA processing, transport, and mRNA decay have been identified. It is apparent like transcription itself, that these steps are also highly regulated (Chen and Shyu 2011, Garneau, Wilusz, and Wilusz 2007). Importantly, changes in mRNA decay rates alter transcript levels and thus affect protein abundance. Moreover, alterations of mRNA stability are reported in several diseases such as cancer, neurodegenerative disease, diabetes, and obesity (Audic and Hartley 2004, Linder, Fischer, and Gehring 2015, Mang et al. 2015). Therefore, the regulation of mRNA decay is receiving attention. Remarkably, it has also become clear that the regulation of mRNA degradation is linked to both transcription and translation (Braun and Young 2014, Collart and Reese 2014, Radhakrishnan and Green 2016).

It is noteworthy that a 5'-3' exoribonuclease, Xrn1, has been proposed to play a key role in mRNA decay-transcription feedback regulation in yeast (Haimovich et al. 2013, Sun et al. 2013, Braun et al. 2014) and also functions in local translation suppression in post synaptic neuron (Luchelli, Thomas, and Boccaccio 2015). In this literature review section, I will briefly explain the main pathway of mRNA decay and the mRNA decay factors involved in each step.

I will also discuss decay-transcription feedback regulation and the coupling mechanism of translation and mRNA degradation. Furthermore, I will review the functions and importance of mRNA decay factors in various physiological phenomena by introducing the studies of loss of function mutations in mRNA decay pathway in model organisms.

1.1 Introduction to mRNA degradation in eukaryotes

Eukaryotic mRNAs have two unique structures, a 7-methyl guanosine cap (m⁷G-cap) structure at the 5' end and a poly(A) tail at the 3' end. These structures provide effective protection against exoribonucleases; hence, these structures are related to mRNA stability (Chen and Shyu 2011, Garneau, Wilusz, and Wilusz 2007). In the normal mRNA degradation pathway, the first step is a shortening of the poly(A) tail, a process called deadenylation. Deadenylation is generally regulated by two distinct deadenylases, Pan2-Pan3 and the Ccr4-Not complex. Pan2-Pan3 is thought to function in the first stage of deadenylation (Yamashita et al. 2005). Pan2 has catalytic activity and belongs to the RNaseD superfamily. However, Pan3 does not have a catalytic domain, so it is thought to be the regulatory subunit (Moser et al. 1997, Parker and Song 2004). When mature mRNAs are transported from the nucleus to the cytoplasm, they have poly(A) tails of approximately 200 – 250 nt. Because this is rather long, in mammalian cells these tails are associated with many poly(A) binding proteins (PABPs). PABPs facilitate the interaction between the poly(A) tail and Pan2-Pan3, and they activate its deadenylase activity. In Pan2-Pan3 mediated deadenylation, poly(A) tails are shortened slowly and synchronously.

This reaction is mediated by the distributive enzyme activity of Pan2-Pan3; thus, after it hydrolyzes just a few nucleotides, it switches the target to another poly(A) tail. Pan2-Pan3 trims poly(A) tails to about 110nt, and subsequently, Pan2-Pan3 dissociates from poly(A) tails because the shortened poly(A) tails bind fewer PABPs. After the dissociation of Pan2-Pan3, the Ccr4-Not complex is recruited to the 3' poly(A) tail and functions in the second stage of deadenylation (Chen and Shyu 2011, Garneau, Wilusz, and Wilusz 2007). The Ccr4-Not complex is a large, multi-subunit protein complex consists of at least 10 core subunits, Cnot1-Cnot3, Cnot6, Cnot6l, and Cnot7-Cnot11 in humans (Shirai et al. 2014). The complex hydrolyzes targeted poly(A) tails nearly completely before switching the target. Therefore, the reaction is asynchronous within each mRNA species. Thus, the second step of deadenylation is often considered the rate-limiting step of mRNA degradation (Chen and Shyu 2011).

Although deadenylated mRNAs are occasionally become re-adenylated and re-enter translation, all mRNAs eventually undergo the next irreversible stage of mRNA decay. After deadenylation, there are two types of irreversible stages. One is decapping, followed by 5' to 3' decay. Decapping is regulated by the Dcp1-Dcp2 complex. Dcp2 possesses a MutT domain, which is commonly found in pyrophosphatases, thus it cleaves the m⁷G-cap, releasing m⁷GDP and a 5' monophosphorylated mRNA body. Initially, Dcp1 was also reported to have decapping activity (LaGrandeur and Parker 1998), however, further studies have shown that it rather functions as an activator of Dcp2 by promoting the formation and stabilization of its active form. (Steiger et al. 2003, She et al. 2008). Finally, deadenylated and decapped mRNAs are degraded by the major cytoplasmic exoribonuclease Xrn1 in a 5' to 3' direction. It is noteworthy

that an additional scaffold protein Edc4 facilitates the interaction between Dcp1 and Dcp2 in metazoans. Moreover, Edc4 also binds to Xrn1, suggesting the coupling of decapping and 5' to 3' mRNA decay (Chang et al. 2014, Braun et al. 2012).

Another irreversible step is 3' to 5' mRNA decay, regulated by exosomes. Exosomes are large protein complexes consisting of 10-12 subunits that form a ring structure. The core subunit of an exosome is Dis3, that belongs to the RNaseII family (Garneau, Wilusz, and Wilusz 2007, Dziembowski et al. 2007). Six subunits (RRP41, RRP42, RRP43, RRP45, RRP46, Mtr3) have RNase PH domains although whether they have a catalytic activity or not is still unclear. The remaining three subunits (RRP4, RRP40, and CSL4) form RNA-binding subunits and share homology with RNA binding proteins, which are classified as either S1 or KH RNA-binding proteins (Allmang et al. 1999). Exosome can also degrade mRNAs having an m7G-cap structure. In this case, the remaining m7G-cap structure is removed from the oligomer by scavenger decapping enzyme Dcps (Liu et al. 2002).

I have reviewed the studies about the two major mRNA degradation pathways and mRNA decay factors (Figure 1.1). More recently, lots of studies have shown that these factors do not only function in mRNA degradation, but also affect mRNA transcription. In the next section, I will introduce recent studies about mRNA decay-transcription feedback regulation with an emphasis on Xrn1, the key regulator of this phenomenon.

a Deadenylation-dependent mRNA decay

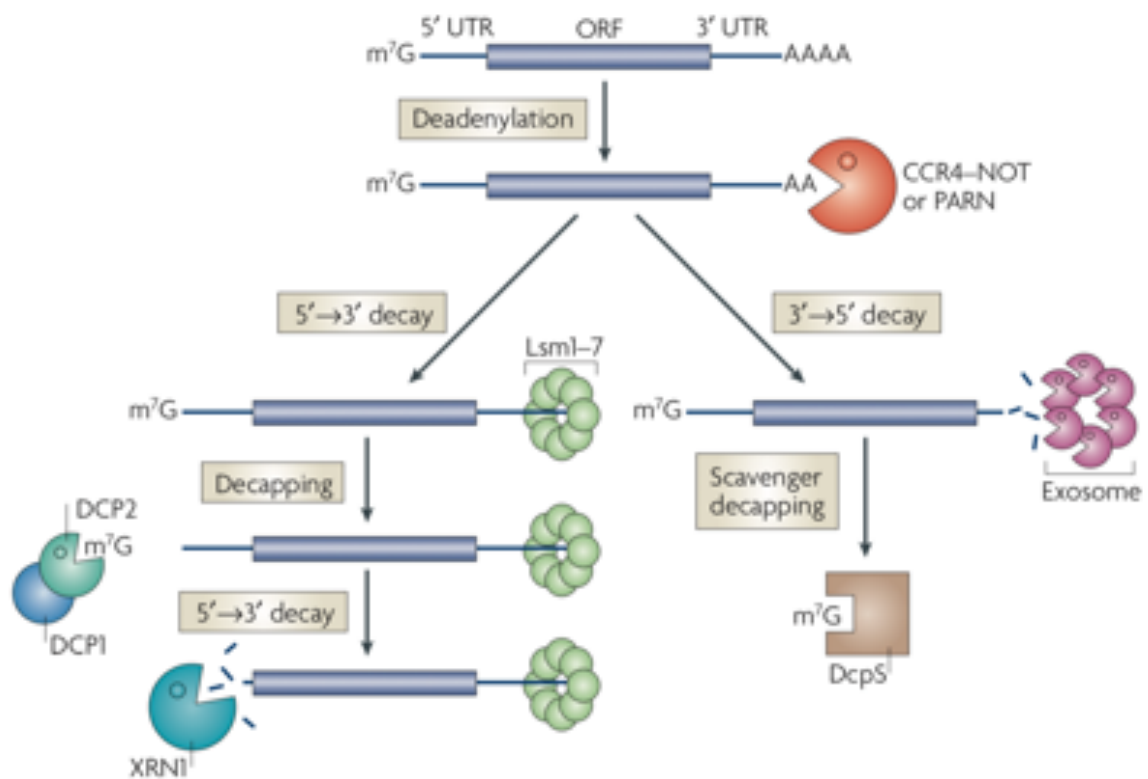


Figure 1.1| The two major mRNA decay pathways in eukaryotes.

Schematic illustration of the two major mRNA decay pathways, a complete description is provided in the main text. Figure adapted from Garneau, Wilusz, and Wilusz (2007)

1.2 Feedback regulation between mRNA degradation and transcription via Xrn1

Transcription occurs in the nucleus and mRNA degradation occurs in the cytoplasm. Since these two events happen in separated cellular compartments, it is understandable that researchers initially did not consider the possibility of coupling mechanisms between transcription and degradation. However, many experimental results have suggested the existence of feedback regulation between transcription and degradation (Collart and Reese 2014). For example, global transcriptome analysis showed that changes in the eventual transcript levels are generally small in mutants having defective mRNA synthesis or mRNA decay (Sun et al. 2012). This indicates that the existence of compensatory mechanisms, since the balance between synthesis and decay determines steady-state mRNA levels. This mechanism is called buffering and is thought to maintain a steady-state level of mRNAs (Collart and Reese 2014).

The first evidence came from the study of yeast Rpb4 and Rpb7, which are dissociable subunits of RNA polymerase II (Pol II) that forms heterodimeric Rpb4/7. The Rpb4/7 heterodimer can bind to mRNAs by interacting with Pol II in the nucleus and they are exported from the nucleus to the cytoplasm together with mRNAs (Choder 2004). A mutation in the core subunit of Pol II that abolishes the interaction of Rpb4/7 with Pol II and mRNAs, impairs transcription and also affects deadenylation of several mRNAs (Lotan et al. 2005).

Additional evidence of coupling between decay and transcription came from the function of the Ccr4-Not complex in transcription initiation and elongation (Collart and Reese 2014, Collart 2016). Not5, a yeast homologue of mammalian Cnot3, interacts with tata-binding

protein (TBP) and TBP-associating factors (TAF). TBP and TAFs are the components of the general transcription factor, transcription factor II D (TFIID), and the integrity of the TFIID is required for the interaction between Not5 and TBP and TAFs, suggesting that Not5 interacts with TBP and TAFs incorporated into TFIID (Badarinarayana, Chiang, and Denis 2000). Also, Not2 interacts with Ada2, a component of SAGA (Spt-Ada-Gcn5 acetyltransferase) complex (Benson et al. 1998, Russell, Benson, and Denis 2002). SAGA complex possesses both histone acetyltransferase and histone deubiquitinase activity, and functions in both transcription activation and transcript elongation (Koutelou, Hirsch, and Dent 2010). In addition, analysis of the Not1 mutant strain in yeast showed that the Ccr4-Not complex is required for precise control of the recruitment of TFIID and SAGA to promoter regions (James, Landrieux, and Collart 2007). Also, it has been reported that Cnot2 and Cnot9 can repress reporter gene activity in human cell lines (Jayne et al. 2006, Zwartjes et al. 2004).

Transcription elongation sometimes causes backtracking of RNA Pol II; therefore, protein complexes called elongation factors (EFs) are required for transcription elongation (Cheung and Cramer 2011). The Ccr4-Not complex is also considered one of the EFs (Collart 2016). Recently, it has been reported that the Ccr4-Not complex binds to the transcription elongation complex via interaction with Rpb4/7 heterodimers in yeast (Babbarwal, Fu, and Reese 2014). Also, the CCR4-NOT complex directly interacts with TFIIS, which is another key molecule of transcription elongation (Dutta et al. 2015, Kruk et al. 2011). From the above, the initial studies about decay-transcription relations focused mainly on Rpb4/7 and the Ccr4-Not

complex. However, three independent groups have newly identified key molecules in the buffering mechanism in yeast (Braun and Young 2014).

Sun et al have developed a new technique called comparative dynamic transcriptome analysis (cDTA) (Sun et al. 2012). cDTA allows for quantitative monitoring of mRNA synthesis rate and decay rate in *Saccharomyces cerevisiae* cells by using *Schizosaccharomyces pombe* cells as a spike-in control. By using this method, Sun et al observed that point mutation in the largest Pol II subunit Rpb1 that impairs transcription leads to a decrease in synthesis rate as predicted, but also a decrease in decay rate. Similarly, they observed that yeast strain lacking deadenylase subunits of the Ccr4–Not complex shows a decrease in decay rate as predicted, but also a decrease in synthesis rate. Based on the cDTA data, they made the extended kinetic model of mRNA turnover. Briefly, they assumed that there is a global transcription modulator and a global degradation modulator that affect the synthesis rate and decay rate, respectively. By analyzing the model, they proposed that decay-transcription feedback is achieved by a factor that functions as a degradation enhancer and a transcription repressor. Previous work showed that both Rpb4/7 and the components of Ccr4–Not complex function as a transcription activator except for Cnot2 and Cnot9, thus they conclude that other factors are required for the buffering system (Sun et al. 2012).

Based on this assumption, Sun et al examined 46 yeast mutant strains lacking mRNA decay factors by cDTA method. 45 out of 46 mutant strains showed buffered total mRNA level. Only the strain lacking the 5' to 3' exonuclease Xrn1 ($\Delta xrn1$) could not buffer the transcript

level. The strain showed 3.2-fold increase in total mRNA levels, because of 2-fold decrease in decay rate and 1.6-fold increase in synthesis rate (Sun et al. 2013).

To clarify whether the increase in synthesis rate observed in $\Delta xrn1$ strain is due to the function of Xrn1 in the nucleus, they used anchor-away technique that allows for pulling out target proteins from the nucleus (Haruki, Nishikawa, and Laemmli 2008). As they expected, Xrn1 anchor-away strain showed increased synthesis rate. Thus, Sun et al assumed that nuclear localized Xrn1 acts as a transcription repressor. However, they could not observe direct interaction between Xrn1 and chromatin by ChIP methods nor direct transcriptional activity of Xrn1 by transcription assay (Sun et al. 2013).

Therefore, they investigated other transcription repressors that may function in a Xrn1-dependent manner and found transcription repressor Nrg1 as one of the buffering machinery (Sun et al. 2013, Vyas et al. 2005). From cDTA results, they found that the synthesis rate of Nrg1 was anti-correlated with the median decay rate of the yeast mutant strains, indicating that Nrg1 is the transcription factor that is induced when decay rate is globally decreased. To clarify the functional relationship between Nrg1 and Xrn1, they overexpressed Nrg1 in both wild type yeast strain and $\Delta xrn1$ strain. The result showed that wild type yeast strain overexpressing Nrg1 showed slow-growth phenotype because of its transcription repressor activity. On the other hand, overexpression of Nrg1 in $\Delta xrn1$ strain did not affect cell growth. Thus, the authors concluded that Xrn1 is required for Nrg1 to function as a transcription repressor. This idea can help understanding of cDTA data set of 46 yeast strains. Yeast strains lacking mRNA decay factors have lower median decay rate, thus Nrg1 synthesis rate is

increased in those strains. Induced Nrg1 functions as a global transcription repressor that eventually leads to reduction of median synthesis rate and thus transcript level would be buffered. However, only $\Delta xrn1$ mutant strain cannot buffer total transcript level because induced Nrg1 cannot work as a transcriptional repressor since $\Delta xrn1$ strain lacks Xrn1 protein. Therefore, Sun et al conclude that Xrn1 functions as a sensor of cellular mRNA decay status and Nrg1 is the effector of the buffering system that tunes the global synthesis rate (Figure 1.2) (Sun et al. 2013).

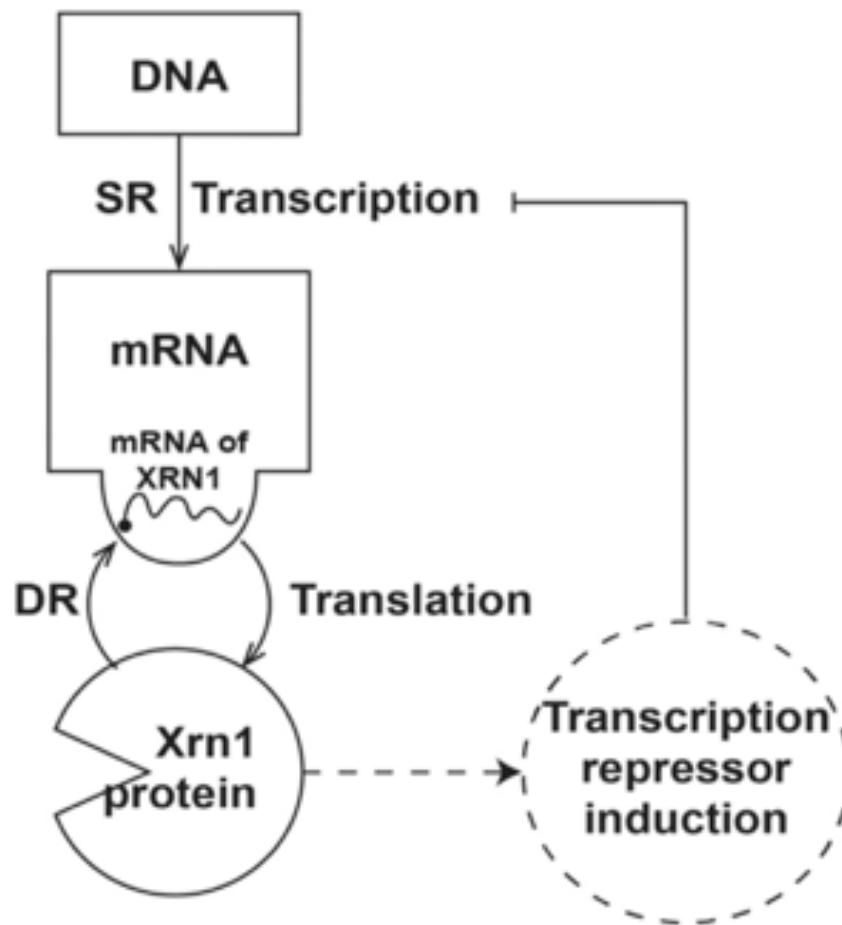


Figure 1.2| Proposed diagram of Xrn1-dependent feedback regulation via indirect activation of transcription repressor.

Complete description is provided in the main text. Figure Adapted from Sun et al. (2013).

At the same time, Haimovich et al also published paper that conclude Xrn1 is the key molecule of decay-transcription feedback mechanism (Haimovich et al. 2013). In this paper, the authors used different method to monitor mRNA decay, synthesis and mRNA abundance compared with Sun et al. For example, mRNA decay was measured by thiolutin shutoff assay that uses transcription inhibitor thiolutin, mRNA synthesis was measured by Genomic run on (GRO) assay, and RNA abundance was measured by microarray analysis. Due to the difference of measurement methods, there was a discrepancy in the data of synthesis rate and RNA abundance of $\Delta xrn1$ mutant strain. In Haimovich's paper, $\Delta xrn1$ mutant strain showed 4.6-fold decrease in synthesis rate and slight decrease in mRNA abundance. Sun et al mentioned about this inconsistency and said that Haimovich's methods were not as accurate as cDTA, because cDTA allows for normalization between different yeast strains and evaluation of absolute changes (Sun et al. 2013).

Based on the decrease of synthesis rate in $\Delta xrn1$ mutant, Haimovich et al assumed that Xrn1 functions as a transcription activator and conducted following research. First, they made mutant strain having point mutation in Xrn1 catalytic domain that abolishes exonuclease activity of Xrn1 (Xrn1^{D208A}) and performed transcription induction assay with various stimulus. The results showed that $xrn1^{D208A}$ strain showed severe defects in transcription induction compared with both wild type and $\Delta xrn1$ strain. Also, they performed Fluorescent in situ hybridization (FISH) analysis to detect specific nuclear transcription sites (TSS) of TEF4 mRNAs in wild type, $\Delta xrn1$ and $xrn1^{D208A}$ strain. They found that in $xrn1^{D208A}$ strain, the fraction of cells having TSS was significantly less compared with wild type. Also, they found

that both $\Delta xrn1$ and $xrn1^{D208A}$ strain showed less intensity of TSs signal compared with wild type, indicating that wild type TSs contained two or more transcript elongating. These results also support the idea that Xrn1 protein functions in transcription initiation and elongation or both (Haimovich et al. 2013).

Next, to investigate functions of Xrn1 in nucleus, they used temperature-sensitive nuclear export mutant ($exp1-1/mex65-5$) and examined nucleocytoplasmic shuttling of mRNA decay factors. Localization analysis using GFP tagged proteins revealed that nuclear localization of enzyme dead $Xrn1^{D208A}$ p was strongly impaired. The authors also generated different mutated Xrn1 proteins, such as $Xrn1^{R101G}$ p and $Xrn1^{H41D}$ p. Both point mutations disrupt the interaction between Xrn1 and decapped RNA, but not enzymatic activity. In addition, they generated $Xrn1^{D208A/R101G}$ p double mutated protein. $Xrn1^{R101G}$ p and $Xrn1^{H41D}$ p showed impaired nuclear localization but not as worse as $Xrn1^{D208A}$ p. Interestingly, $Xrn1^{D208A/R101G}$ p could partially rescue the nuclear localization ability compared with $Xrn1^{D208A}$ p, suggesting $Xrn1^{D208A}$ p sticking to decapped mRNA without degrading it. It is noteworthy that nuclear import of RFP tagged Dcp2 was also strongly impaired in $xrn1^{D208A}$ cells, indicating that Xrn1 enzymatic activity is also required for the shuttling of some other mRNA decay factors (Haimovich et al. 2013).

Since all tested mRNA decay factors can shuttle from the nuclear to the cytoplasm, Haimovich et al performed ChIP assay to examine whether mRNA decay factors (Xrn1-TAP, Dcp2-TAP, and Lsm1-TAP) can directly bind to chromatin or not. Unlike Sun's paper, Haimovich could detect direct interaction between these decay factors and chromatin.

Intriguingly, these decay factors associated preferentially with transcription start-sites of genes coding unstable mRNAs or having high transcription rate. They also performed in vitro tethering assay using decay factors fused with Gal4 DNA binding domain (Gal4-BD). The result showed that Ccr4, Dcp2, Dhh1 and Pat1 could activate transcription, indicating that these decay factors might have activator domain. Interestingly, enzyme dead form Dcp2-4p also activated transcription. Thus, at least Dcp2, does not require enzymatic activity to function as a transcriptional activator. Moreover, they also reported that Gal4-BD-Dcp2 could not activate transcription in the case of both $\Delta xrn1$ and $xrn1^{D208A}$ cells, suggesting that Xrn1 is required for transcriptional activity of some decay factors, like as the case of Nrg1 in Sun's paper (Haimovich et al. 2013).

Haimovich also examined whether Xrn1 deletion has some effects on transcription elongation. They performed RNA Pol II ChIP-on-chip (RPCC) using a membrane containing 5' and 3' probes to detect relative Pol II distribution in 5' area and 3' area. Also, they performed Genomic run-on (GRO) to detect active Pol II fraction in 5' area and 3' area. Their data revealed that in Xrn1 mutant strain ($\Delta xrn1$ and $xrn1^{D208A}$), Pol II was accumulated in 3' region of the genes. However, GRO did not show biased signal in those mutants, indicating that accumulated Pol II in mutant strains were not elongating. To confirm this observation, they also examined phosphorylation status of Pol II (Ser2P-CTD), which is often used as an indicator of elongating Pol II. The results clearly showed that phosphorylation of Ser2-CTD was reduced in Xrn1 mutants, suggesting that deletion or disruption of Xrn1 has some impact to Pol II elongation activity (Haimovich et al. 2013). They found that including Xrn1, deletion of decay factors

causes downregulation of transcription. All examined decay factors have nucleocytoplasmic shuttling ability and shuttling ability of some decay factors is impaired when the function of Xrn1 is disrupted. Also, several decay factors bind to transcription start sites of genes coding unstable mRNAs or having high transcription rate and Xrn1 is required for the transcriptional activity of some decay factors. Therefore, they conclude that Xrn1 is the key molecule of mRNA decay-transcription feedback loop and some mRNA decay factors function as transcription activator by shuttling from the cytoplasm to nucleus after they degrade mRNAs (Figure 1.3) (Haimovich et al. 2013).

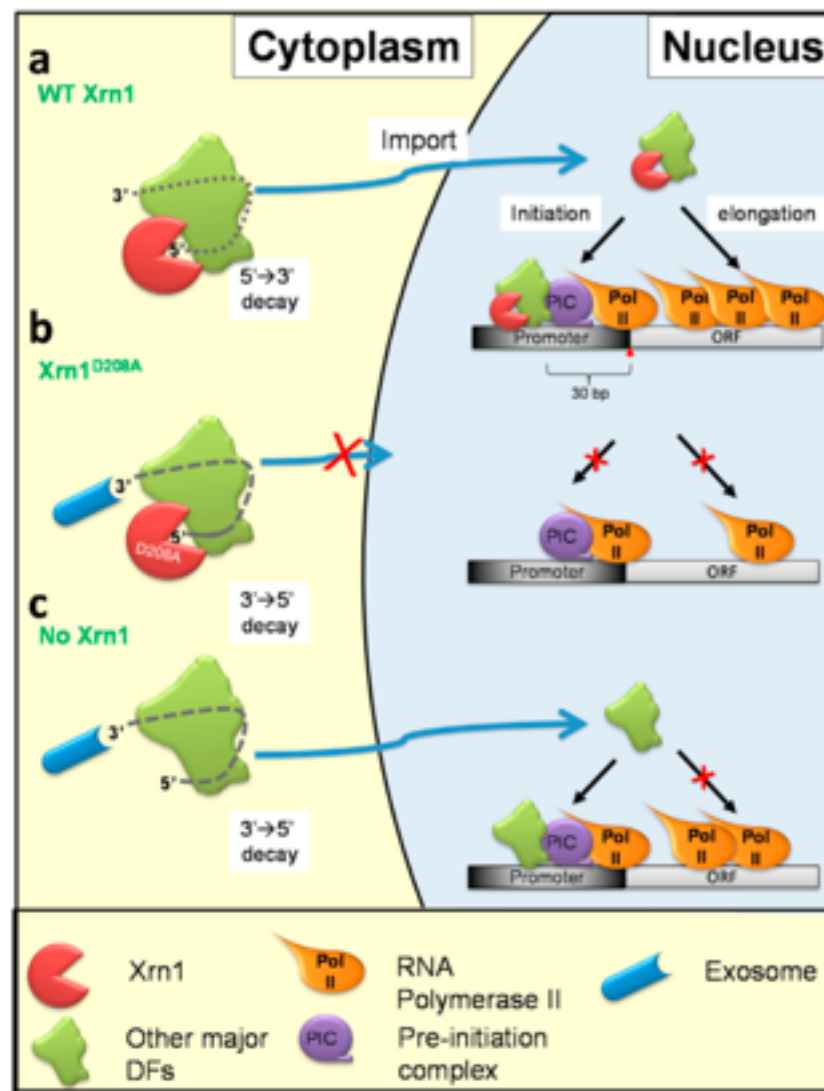


Figure 1.3| Proposed diagram of Xrn1-dependent feedback regulation and nucleocytoplasmic shuttling of mRNA decay factors.

Complete description is provided in the main text. Figure adapted from Haimovich, G et al. (2013).

The key difference of Sun and Haimovich's paper was the results of synthesis rate in $\Delta xrn1$ strain. For example, Sun's data showed $\Delta xrn1$ strain had 1.6-fold increased synthesis rate. Hence, they assumed that Xrn1 functions as transcription repressor, and conduct following research. On the other hands, Haimovich's data showed $\Delta xrn1$ strain had 4.6-fold decreased synthesis rate. Thus, they assumed that Xrn1 functions as transcription activator. This difference might be due to the difference of methods they took. In addition, their ChIP assay results was also inconsistent. Sun could not detect the direct interaction between Xrn1 and chromatin, but Haimovich could. From the above, it is likely that Xrn1 is a key molecule of the feedback regulation. However, whether Xrn1 functions as a transcription activator or repressor, and whether Xrn1 directly binds to chromatin and affect transcription or indirectly control transcription via other molecules such as Nrg1 are remains to be elucidated.

Both Sun and Haimovich's group used yeast grown in the high glucose condition. Another group has studied mRNA decay-transcription feedback regulation in a glucose depleted condition. Under stress conditions such as glucose depletion, cells regulate gene expression through both transcriptional and post-transcriptional regulation and adopt to new environments. Snf1, the *Saccharomyces cerevisiae* ortholog of adenosine monophosphate-activated protein kinase (AMPK), signaling pathway is activated by glucose depletion and enabling adaptive cellular responses. Braun et al. performed phosphoproteomics analysis and identified Xrn1 as a Snf1-dependent phosphorylated protein (Braun et al. 2014). Moreover, they found that Xrn1 is required for transcription and glucose-induced mRNA decay of Snf1-dependent genes (Braun et al. 2014).

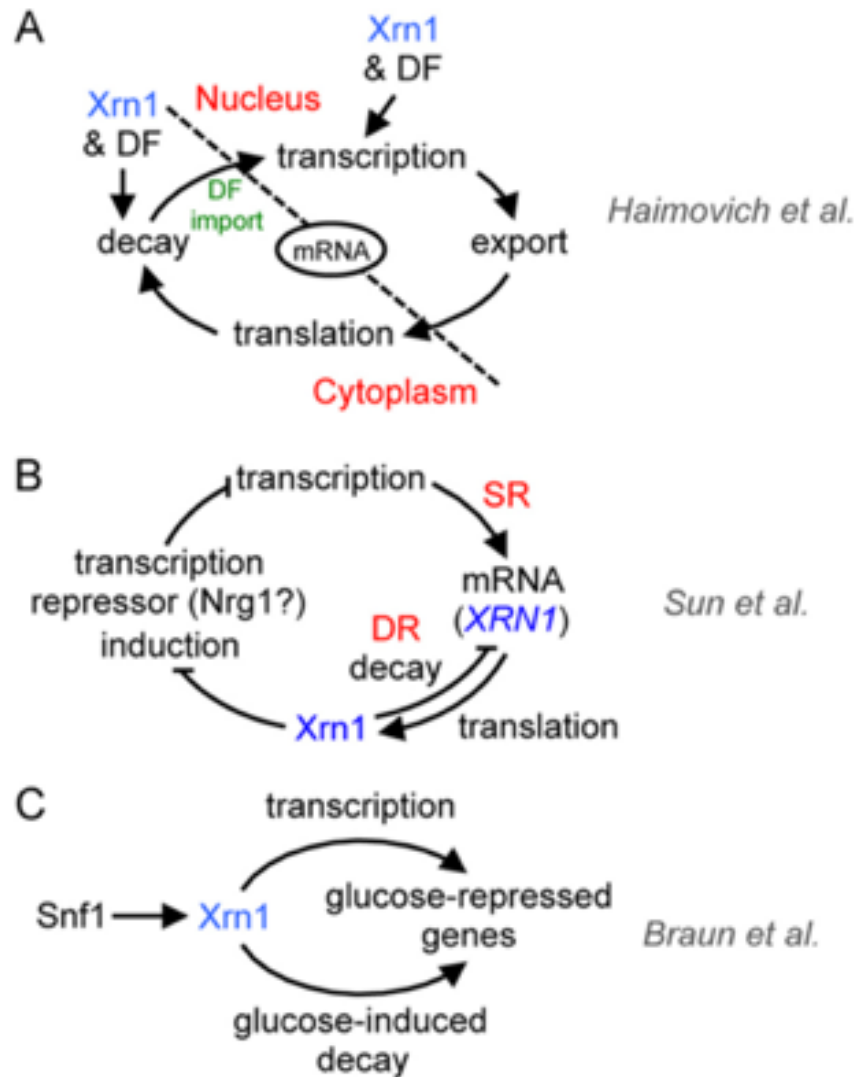


Figure 1.4| Xrn1 mediated mRNA decay-transcription feedback models proposed by three different groups.

Schematic illustration of the circular regulation of transcription and mRNA degradation. Complete description is provided in the main text. Figure adapted from Braun and Young (2014)

Compared with outcomes in yeast, research about mRNA decay-transcription feedback mechanisms in mammals has not progressed very far. Recently, Abernathy et al. reported that Xrn1-dependent feedback regulation is conserved in mammals (Abernathy et al. 2015). In addition, they also found that changes in mRNA degradation are somehow sensed in order to activate transcriptional changes. The authors examined the effects of a cytoplasmic mRNA-targeting viral endonuclease, SOX. Gamma-herpesviruses encode this protein and it cleaves most cellular mRNAs. Thus, either infection with the virus or expression of the viral protein in mammalian cell lines accelerates mRNA decay. Importantly, mRNA decay caused by viral nucleases requires host Xrn1 protein to eliminate cleaved mRNAs. Therefore, the authors considered the possible relationship between viral infection and Xrn1-mediated feedback regulation.

Briefly, their results showed that accelerated mRNA decay triggered by viral nucleases leads to repression of transcription of host genes, but viral genes can escape this transcriptional repression, so the Xrn1-dependent feedback mechanism is beneficial to viruses, suggesting that Xrn1-dependent feedback is also important for physiological mechanisms in mammals.

1.3 mRNP granules and local translation regulation

After transcription, mRNAs are exported to cytoplasm and used as a template of translation then degraded. These processes are organized and controlled by various mRNA binding proteins and non-coding RNAs. Under certain condition, these factors and mRNAs form

membrane less cytoplasmic foci known as messenger ribonucleoprotein particles (mRNPs) (Parker and Song 2004). mRNAs incorporated into mRNPs are either be degraded or translationally suppressed. mRNPs are classified based on the difference in the composition and the formation process (Buchan and Parker 2009). Most well studied mRNPs are processing bodies (P-bodies) and stress granules. P-bodies contain mRNA decay machineries such as the CCR4-NOT complex, decapping complex, and Xrn1. However, it does not contain ribosomal subunits and poly A binding proteins (PABPs) suggesting that P-bodies mainly functions as the place for deadenylation dependent mRNA decay. On the other hands, stress granules contain translation initiation factors (eIF4E, eIF4G, eIF4A, eIF3, and eIF2), PABPs, and 40S ribosomal subunits. mRNAs associated with stress granules are translationally silenced, but they can re-enter into translation when translation arrest is relieved (Parker and Song 2004, Buchan and Parker 2009).

It is noteworthy that Xrn1 was the first mRNA degradation factor detected in cytoplasmic foci in mouse cells (Bashkirov et al. 1997). Xrn1 is detected both in P-bodies and stress granules (Buchan and Parker 2009, Thomas et al. 2009). mRNPs are not only controlling the mRNA decay and translation, but also play important roles in mRNA transport. mRNA transport and local translation modulate neuronal development. Neuronal granules contain mRNA transport related protein Staufen that is thought to mediate translational repression and/or mRNA transport in neuronal cells (Kiebler and Bassell 2006). In *Drosophila*, Pacman, which is the ortholog of Xrn1, is found in neuronal transport granules (Barbee et al. 2006). Also, Luchelli et al. have shown that Xrn1 forms unique cytoplasmic foci at the post synapse of rat's

hippocampal neuron (Luchelli, Thomas, and Boccaccio 2015). They named it synaptic XRN1 bodies (SX-bodies) and found that SX-bodies are different from other RNA granules such as P-bodies, stress granules, and other known neuronal granules in terms of the composition and the forming process. At the post synapse, the RNA regulator Smaug1 and Fragil X Mental Retardation Protein (FMRP) containing cytoplasmic foci are observed and they are called S-foci and FMRP granules, respectively. S-foci and FMRP granules regulate the mRNA stability and local translation at the post-synapse. Previous studies have shown that NMDAR stimulation triggers the dissolution of S-foci but does not affect the number and size of FMRP granules. On the other hand, the activation of metabotropic glutamate receptors mGluR triggers the rapid dissolution of the S-foci and FMRP granules (Thomas and Boccaccio 2016). The SX-bodies do not contain Dcp1a, Smaug, and FMRP, suggesting that they are different from canonical p-bodies, S-foci, and FMRP granules. Moreover, in contrast to other neuronal granules, SX-bodies increase in size and number upon NMDAR stimulation, which triggers a global translational silencing (Luchelli, Thomas, and Boccaccio 2015). These results clearly showed that SX-bodies are unique and Xrn1 should have key roles in local translation of mRNAs under the specific stimuli at post synapse, although the target transcripts of the local translation suppression are still unknown (Figure 1.5) (Thomas and Boccaccio 2016).

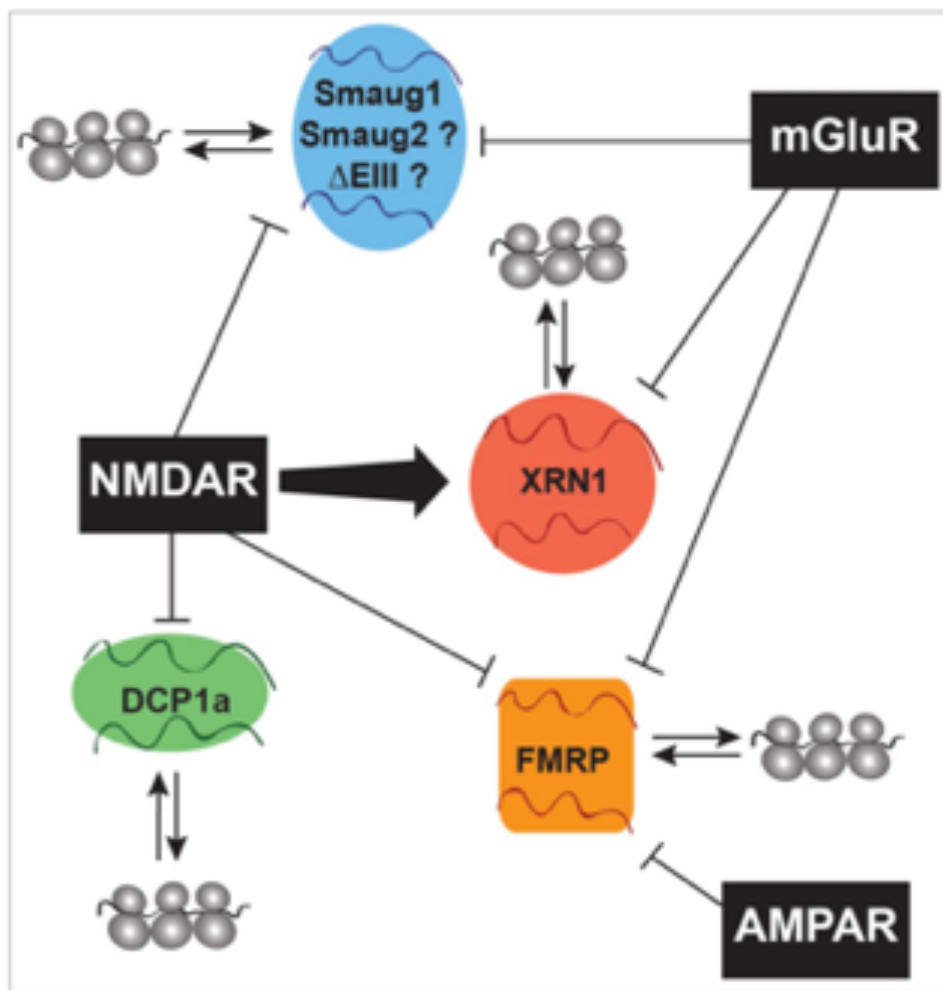


Figure 1.5| Comparison of different mRNA silencing foci at post synapse under various stimuli.

Schematic illustration of the dynamics of RNA granules upon different stimuli. Complete description is provided in the main text. Figure adapted from Thomas and Boccaccio (2016)

1.4 Role of mRNA degradation in physiology

mRNA degradation factors have multifunctional roles in gene expression process. Thus, they are also responsible for various physiological phenomenon. In this section, I will focus on findings in knockout models of mRNA degradation factors mainly in mammalian systems and will occasionally refer to findings from non-mammalian systems.

The Ccr4-Not complex is one of the most well-studied mRNA degradation factors in mammalian systems. The subunits of the CCR4–NOT complex are ubiquitously expressed in adult mice with some tissue preferences, such as brain, testis, and metabolic tissues (Chen et al. 2011). Depletion of Cnot1, Cnot2, and Cnot3 causes cell death such as apoptosis and necroptosis in mammalian cells. (Ito, Takahashi, et al. 2011, Ito, Inoue, et al. 2011, Suzuki et al. 2015). Also, homozygous knockout of some subunits of the CCR4-NOT complex leads to embryonic lethality (Shirai et al. 2014, Morita et al. 2011). Muscle specific depletion of Cnot1 and Cnot3 causes heart failure via upregulation of the key autophagy regulator Atg7 (Yamaguchi et al. 2018). Cnot3 is also required for B cell development (Inoue et al. 2015), bone mass metabolism (Watanabe et al. 2014), and postnatal liver function maturation (Suzuki et al. 2019). In addition, Cnot7, a catalytic subunit of the CCR4-NOT complex, is essential for male fertility (Berthet et al. 2004, Nakamura et al. 2004). Importantly, the CCR4-NOT complex is regulating energy homeostasis in liver and adipose tissues via controlling the stability of specific mRNAs (Morita et al. 2011, Takahashi et al. 2015, Morita et al. 2019, Takahashi et al. 2019, Salem et al. 2019).

Compared to the deadenylation complex, physiological studies in decapping enzymes and exonucleases are limited. Mutations in DCAP-1 and DCAP-2, which are the homologues of DCP1-DCP2 decapping complex in *C. elegans*, reduce longevity and stress resistance in *C. elegans* (Rousakis et al. 2014) and this phenotype is rescued by expressing DCAP-1 specifically in neuronal cells (Borbolis et al. 2017). This result suggests that decapping complex plays important roles in neurons to regulate specific genes related to stress resistance and life span in worm. On the other hand, DCP2 hypomorphic knockout mice are fertile, viable, and grow normally compared to their littermates (Song, Li, and Kiledjian 2010). In yeast, disruption of 5' to 3' exoribonuclease Xrn1 causes severe growth defect (Larimer and Stevens 1990). siRNA-mediated knockdown of Xrn1 in *C. elegans* causes embryonic lethality due to the failure of ventral epithelial enclosure during embryogenesis (Newbury and Woollard 2004). Interestingly, hypomorphic mutations in Pacman, which is the homologue of XRN1 in *D. melanogaster*, also causes defect in dorsal/thorax closure and epithelial sheet sealing that is relevant to ventral epithelial enclosure in *C. elegans* (Grima et al. 2008, Jones, Zabolotskaya, and Newbury 2012). Mutations in Pacman also causes defects in spermatogenesis and oogenesis, thus XRN1 is required for male and female fertility in *D. melanogaster* (Zabolotskaya et al. 2008, Lin et al. 2008). In mouse testis, XRN1 is recruited to the transcripts having m⁶A modification by YTHDC2, a YTH domain containing m⁶A reader protein, and thus involving in spermatogenesis (Wojtas et al. 2017). As these studies showed, mRNA degradation is important for various physiological phenomena. However, further analysis is necessary to understand the roles of its individual factors in tissue function and homeostasis.

1.4 Aim of the study

I have briefly introduced the main pathway and function of mRNA degradation systems. Also, I have reviewed mRNA decay-transcription feedback regulation and local translation control via mRNPs. In each section, I have shown that Xrn1 has important roles, however, there has been no knockout mouse studies of XRN1. Therefore, the main aim of my project is to elucidate the functional role of Xrn1 in mouse physiology by generating and analyzing Xrn1 knockout mice. In addition, several studies have already shown that Xrn1 must play important roles in neurons and brain, thus I will establish brain specific Xrn1 conditional knockout mice and analyze its phenotypes to elucidate the physiological role of Xrn1 in mouse brain.

Chapter 2 Materials and Methods

2.1 Mice

Xrn1^{fllox/+} mice were generated by ssODN (single-strand oligodeoxynucleotides)-mediated knock-in with CRISPR-Cas in C57BL/6N zygotes in which loxP sites flank exons 2 and 6 of the *Xrn1* gene (accession no. CDB0007E, RIKEN). Two gRNAs and ssODN targeting intron 1 and intron 6 of the *Xrn1* gene, and Cas9 were injected into wild type zygotes. The gRNA and ssODN sequences were listed in Table 2.1. Confirmation of loxP insertion in cis orientation was performed by genotyping in F1 offspring. Primers used for detection of wild type and floxed alleles are listed in Table 2.2.

CAG-Cre mice that express Cre recombinase gene under the control of the cytomegalovirus immediate early enhancer-chicken b-actin hybrid (CAG) promoter were used to generate whole-body knockout mice of *Xrn1*. To generate whole-body knockout mice of *Xrn1*, we crossed *Xrn1^{fllox/flox}* mice with *CAG-Cre^{+/-}* mice. Primers used for detection of wild type, floxed, and knockout alleles are listed in Table 2.2.

Camk2a-Cre mice that express Cre recombinase gene under the control of the mouse calcium/calmodulin-dependent protein kinase II alpha (*Camk2a*) gene promoter were used to generate forebrain specific knockout mice of *Xrn1*. To generate forebrain specific knockout mice of *Xrn1*, we crossed *Xrn1^{fllox/flox}* mice with *Xrn1^{fllox/+}*, *Camk2a-Cre^{+/-}* mice. Primers used for genotyping of wild type and floxed alleles are listed in Table 2.2. All mice used were maintained under a 12-hr light/12-hr dark cycle in a temperature- controlled (22°C) barrier

facility with free access to water and normal chow diet (NCD, CA1- 1, CLEA Japan). The gender and age of mice used for experiments were indicated in the figure legends. Mouse experiments were approved by the animal experiment committee at the Okinawa Institute of Science and Technology Graduate University (OIST).

2.2 Genotyping

Tails from 3 weeks old mice were lysed in 50 μ l of DNA extraction solution 1 (25 mM NaOH, 0.2 mM EDTA) for 20 minutes at 95°C. Followed by addition of 50 μ l of DNA extraction solution 2 (40 mM Tris-HCl pH 5.0). Samples were vortexed and spin downed by tabletop centrifuge. 0.5 μ l of the lysate was used as a template for PCR amplification. All genotyping primers are listed in Table 2.2.

PCR mixture:

10x NH ₄ reaction buffer	2 μ l
2.5 mM dNTP	2 μ l
50 mM MgCl ₂	1.2 μ l
BIOTAQ DNA Polymerase	0.1 μ l
10 μ M of primer (reverse + forward)	0.5 μ l
template DNA	0.5 μ l
ddw	13.7 μ l

PCR amplification cycle of genomic DNA (Step 2 to Step 4 was repeated for 35 cycles)

- Step1 2 minutes at 95 °C
- Step2 30 sec at 95 °C
- Step3 30 sec at 60 °C
- Step4 45 sec at 72 °C
- Step5 5 minutes at 72 °C

PCR products were run on 2% agarose gel with 2x loading sample buffer.

2.3 Daily food intake analysis

Prior to measuring daily food intake, animals were single-caged and kept under a normal 12-hr light-dark cycle. At least after 1 day of acclimation, the weight of food supplied was measured. 24 hours after, the weight of food remaining was measured again. The value of subtraction of the weight of food remaining from the weight of food supplied was used as daily food intake.

2.4 Blood analysis

Random blood glucose was measured from tail vein blood using glucometer (Glutest Neo Sensor, Sanwa Kagaku Kenkyusho). The mice used for collecting serum were euthanized by isoflurane, and blood was taken from inferior vena cava. Whole blood was kept at room temperature until forms clot, then centrifuge at 2000g for 10 minutes to separate serum.

Concentrations of serum insulin and serum leptin was measured by Mouse Insulin ELISA kit (Merckodia) and Mouse Leptin ELISA kit (ab199082, Abcam).

2.6 Metabolic analysis

6-7-week-old mice were acclimated for 3 days in a metabolic chamber with food and water under a normal 12-hr light-dark cycle. Oxygen consumption (VO_2), carbon dioxide production (VCO_2), respiratory exchange ratio (RER), and energy expenditure were measured after acclimation with an Oxymax system (CLAMS; Columbus Instruments, Columbus, OH, USA). For home cage activity monitoring, mice (6-8 weeks of age) were housed individually in cages with a lid containing CCD camera and white and IR LED unit (O'HARA & CO.,LTD.) under a normal 12-hr light-dark cycle and had free access to both food and water. After 1-day acclimation, the subject's distance traveled in every minute was measured with the software (O'HARA & CO.,LTD.).

2.7 Immunoblotting

For protein expression analysis, the mice were euthanized by isoflurane and perfused with PBS. The tissue was frozen in liquid nitrogen immediately after excision and kept in $-80^{\circ}C$ until used. The tissue was homogenized in TNE buffer (20 mM Tris-HCl (pH 7.5), 150 mM NaCl, 2 mM EDTA, 1% NP40, EDTA free Protease Inhibitor Cocktail (Nakarai Tesque), 1 mM PMSF, 1mM β -Glycerophosphate, 1mM Na_2VO_3 , and 1mM NaF) by passing the tissue in lysis buffer

10 times through a 24 G needle and incubated for 30 minutes on ice. Lysate were clarified by centrifugation at 16,000 g for 10 min at 4°C. Protein concentration in the lysate was measured using Pierce BCA protein assay Kit (Thermo Fisher Scientific) and dissolved in 1XSDS sample buffer (containing 3% SDS, 10 % glycerol, and 5% β -mercaptoethanol). Proteins in the lysate were then reduced through boiling on heat block for 5 minutes at 95°C and subjected to SDS-polyacrylamide gel (SDS-PAGE) electrophoresis. Afterward, proteins separated on the SDS-PAGE were electro-transferred onto 0.45 μ m polyvinylidene difluoride membranes (PVDF, Millipore cat no. IPVH00010) using wet transfer system (Nihon Eido, Tokyo, Japan). After the membranes were blocked with 3% skim milk/TBST (20 mM Tris-HCl, pH 7.5, 150 mM NaCl, 0.5% v/v Tween 20), proteins of interest were probed with appropriate specific primary antibodies and then horse radish peroxidase (HRP)-conjugated secondary antibodies against the primary antibodies' host. Chemiluminescent signals were detected using an ImageQuant LAS 4000 mini (GE Healthcare, Tokyo). Sequential probing of the membranes with a variety of antibodies was performed after inactivation of HRP with 0.1% sodium azide (NaN_3), according to the antibody manufacturer's protocol. Protein level was quantified using ImageJ software and normalized to α -tubulin.

2.8 Antibodies for immunoblotting

The following primary antibodies were used: XRN1 (1:5000 in Can Get Signal Solution 1 (Toyobo); A300-443A; Bethyl Laboratories), LEPR (1:1000 in CGS Solution 1; ab177469; Abcam), JAK2 (1:1000 in CGS Solution 1; #3230S; Cell Signaling Technology), STAT3 (1:1000 in CGS Solution 1; #4904S; Cell Signaling Technology), SOCS3 (1:1000 in CGS Solution 1; #2923S; Cell Signaling Technology), IRS1 (1:1000 in CGS Solution 1; 611394; BD Transduction Laboratories), PI3K (1:1000 in CGS Solution 1; #4292S; Cell Signaling Technology), AKT (1:1000 in CGS Solution 1; #9272S; Cell Signaling Technology), Foxo1 (1:1000 in CGS Solution 1; #2880S; Cell Signaling Technology), PTEN (1:1000 in CGS Solution 1; #9559S; Cell Signaling Technology), α -Tubulin (1:1000 in 3% skim milk/TBST; #T9026; Sigma), and GAPDH (1: 1000 in 3% skim milk/TBST; #2118; Cell Signaling Technology).

The following secondary antibodies were used: ECL anti-mouse IgG HRP-linked whole antibody (from sheep) (1:3000 in CGS Solution 1; NA931V; GE healthcare), ECL anti-rabbit IgG HRP-linked whole antibody (from donkey) (1:3000 in CGS Solution 1; NA934V; GE healthcare)

2.9 Quantitative real-time RT-PCR (qRT-PCR)

For qRT-PCR analysis, the mice were euthanized by isoflurane and perfused with PBS. The tissue was frozen in liquid nitrogen immediately after excision and kept in -80°C until used.

Total RNA was isolated from the tissue by using 1 ml of ISOGEN II (Nippon gene). 1 μg of total RNA was used for cDNA synthesis with SuperScript Reverse Transcriptase III (Thermo

Fisher Scientific) as follows:

Mixture 1:

Total RNA	1 μg
Oligo(dT) 12-18 primers	1 μl
2.5 mM each dNTP	4 μl
ddw	Up to 13 μl

Mixture 1 was boiled at 65 degrees for 5 minutes followed by at least 1 minute on ice. Then mixture 2 was added.

Mixture 2:

5x First Strand buffer	4 μl
0.1 M DDT	1 μl
RNaseOut	1 μl
SuperScript III RT	1 μl

Tubes were incubated in PCR thermal cycler with the following conditions: 50°C for 1 hour and 70°C for 15 minutes. cDNA was diluted 10-fold with RNase-free water. Generated cDNA was kept at -20 till further analysis.

For qRT-PCR, reactions were performed using 2.5 μ l of cDNA1, 5 μ l of SYBR Premix Ex Taq (Takara), 0.2 μ l of ROX II reference dye, 0.2 μ l of 10 μ M primer (reverse + forward). qRT-PCR reactions were performed using primers listed in Table 2.1 and analyzed with a Viia7 sequence detection system (Applied Biosystems). Each sample was run in two technical replicates using the following PCR conditions:

PCR amplification cycle of cDNA (Step 2 to Step 4 was repeated for 40 cycles)

- Step1 95°C for 30 seconds
- Step2 95°C for 5 seconds
- Step3 60°C for 30 seconds
- Step4 75°C for 15 seconds
- Step5 60°C for 1 minute
- Step6 95°C for 15 seconds

Relative expression of mRNA was determined after normalization to *Gapdh* mRNA using the $\Delta\Delta C_t$ method.

2.11 Immunohistochemistry

11-week old male mice were euthanized by isoflurane and perfused with 4% PFA/PBS. After perfusion, the brains were dissected and further fixed in 4% PFA/PBS overnight at 4°C. The fixed brains were soaked in 15% sucrose/PBS for 2 hours at 4°C and 30% sucrose/PBS overnight at 4°C. The brains were embedded in Optimal cutting temperature (OCT) compound and frozen at -20°C. The frozen brains were coronally sectioned at 30 µm using a Cryostat (Leica CM 3050S). The brain sections were kept in PBS at 4°C till used. The brain sections were mounted onto coated slides, then washed two times with PBS. After the slides were blocked with blocking buffer (PBS with 0.5 % Triton X-100 and 5% goat serum) for 1 hour at RT, they were incubated with either Pomc antibody (1: 250 in blocking buffer; H-029-30; Phoenix Pharmaceuticals) or AgRP antibody (1: 250 in blocking buffer; H-003-57; Phoenix Pharmaceuticals) at 4°C overnight. After several rinses in PBS-T (PBS with 0.5 % Triton X-100), slides were incubated with secondary antibody (Goat Anti-Rabbit IgG H&L (Alexa Fluor® 555); ab150078; Abcam) for 2 hours at RT. Slides were then rinsed in PBS-T and incubated with DAPI. Fluorescent signals of secondary antibody and DAPI were detected by fluorescent microscopy BZ-X700 (Keyence). Obtained images are further analyzed using ImageJ software to quantify the signal intensity and cell numbers.

2.10 Proteomics analysis

11-week old male mice were euthanized by isoflurane and perfused with PBS. The hypothalamus was frozen in liquid nitrogen immediately after excision and kept in -80°C until used. The hypothalamus was homogenized in TNE buffer (20 mM Tris-HCl (pH 7.5), 150 mM NaCl, 2 mM EDTA, 2 mM MgCl_2 , 2% SDS, 1% NP40, EDTA free Protease Inhibitor Cocktail (Nakarai Tesque), 1 mM PMSF, 1 mM β -Glycerophosphate, 1 mM Na_2VO_3 , and 1 mM NaF) by passing the tissue in lysis buffer 10 times through a 24 G needle. Following sonication, samples were centrifuged at 16,000 g for 10 min. Proteins in the lysate were reduced with DTT (final concentration of 10 mM) through boiling on heat block for 30 minutes at 60°C and alkylated using iodoacetamide (final concentration of 50 mM) for 30 min at room temperature in the dark. Protein concentration in the lysate was measured using Direct Detect assay-free cards with the Direct Detect spectrometer (Merck Millipore).

For the gel-based digestion protocols, tissue lysate containing 10 μg of protein was mixed with LDS buffer and resolved on NuPage 4–12% Bis-Tris protein gels (Invitrogen). The gel was fixed in 50% methanol and 10% acetic acid for 1 hour, then stained with NOVEX Colloidal Blue Staining Kit (Invitrogen) for 3 h. After staining, the gel was washed with distilled water. The gel images were taken by ChemiDoc XRS Plus (Bio-Rad). Protein gel was excised into 8 pieces per lane and destained by soaked in 25 mM ammonium bicarbonate/50% methanol for 4 times. After dehydration by acetonitrile (ACN), the proteins in the gel pieces were digested overnight at 37°C with digestion buffer (5% acetonitrile, 25 mM ammonium

bicarbonate, 2 mM CaCl₂) containing 250 ng of trypsin (Promega). Trypsin-digested peptides were extracted by sequential wash with 1.25% trifluoroacetic acid (TFA)/50% ACN, 0.33% trifluoroacetic acid (TFA)/66% ACN, and 100% ACN. The elute containing peptides was evaporated by EZ-2 Elite evaporator (Genevac). To purify the eluted peptides, handmade stage-tip was used. 4 pieces of Empore disks (3M Empore High Performance Extraction Disk) were inserted into 200 µL micropipette tips. Before loading the sample, the stage-tip sorbents were activated with 50 µl of methanol (1600g, 3min, RT), cleaned with 50 µl of 0.1% TFA/60% ACN (1600g, 3min, RT), and equilibrated with 200 µl of 0.1% TFA (1600g, 9min, RT). The samples were resuspended in 50 µl of 1% TFA, then loaded to the stage-tip (1600g, 5min, RT). The stage-tips containing peptides were washed twice with 200 µl of 0.1% TFA (1600g, 6min, RT) and peptides were eluted twice with 50 µl of 0.1% TFA/60% ACN (1600g, 3min, RT). The elute containing peptides was evaporated by EZ-2 Elite evaporator (Genevac) and resuspended in 25 µl of 0.1% TFA. The peptide resuspension was analyzed by LC/MS/MS, using nano-Acquity LC (Waters) connected to Orbitrap Fusion Lumos (Thermo Fisher Scientific). Obtained mass spectrometry data was analyzed using ProteomeDiscoverer 2.2 software (Thermo Fisher Scientific).

2.17 Primers

Table 2.1| gRNA and ssODN used for *Xrn1*^{flox/+} mice generation.

Type/name	Sequence (5'-3')
5'gRNA	CAATAATCACCGTCGAATAAAGG
3'gRNA	AAGTGTAGCTCAGCAGCCGGGGG
5'ssODN	AAAAACAAACCTTAATAAACTTCAATAATCACCGTCGAAGATATCATAACTTCGTATAG CATACATTATACGAAGTTATTAAGGAGGTAAAGGGAAGCCAATAGGAACGGCTAGTAAT
3'ssODN	CCTAGGTTAAGACCACAGAACCCAAGTGTAGCTCAGCAGCGATATCATAACTTCGTATAGC ATACATTATACGAAGTTATCGGGGGCTCACCTTGGGGCCCAGCCAGTCCTGCCAAAAT

Table 2.2| Primer sets used for genotyping.

Target	Primer sequence (5'-3')	Expected size
<i>Xrn1</i>	5' Fw2: GTCTCTCCATTACTAGCCGTTCC 5' Re2: CTGTGTACAACCTGCATCTCC 3' Re: CATGCTTTTCTGAGACCC	WT:204 Flox:244 KO:421
CAG-Cre	Cre Fw: TCGATGCAACGAGTGATGAG Cre Re: TTCGGCTATACGTAACAGGG IL-2 Fw: CTAGGCCACAGAATTGAAAGATCT IL-2 Re: GTAGGTGGAAATTCTAGCATCATCC	Cre: 482 IL-2: 324
Camk2a-Cre	Cre Fw: GAGGGACTACCTCCTGTACC Cre Re: TGCCCAGAGTCATCCTTGGC IL-2 Fw: CTAGGCCACAGAATTGAAAGATCT IL-2 Re: GTAGGTGGAAATTCTAGCATCATCC	Cre: 630 IL-2: 324

Table 2.3| Primer sets used for qPCR

Gene symbol	Fforward primer (5'-3')	Reverse primer (5'-3')
mAgrp	AGAAGACAACACTGCAGACCGAG	GTTCTGTGGATCTAGCACCTCC
mAkt1	GTGGCAGGATGTGTATGAGAAG	ACCTGGTGTCACTCTCAGAGG
mCart	GGACATCTACTCTGCCGTGG	TCGATCTGCAACATAGCGCC
mFoxo1	GCTGGGTGTCAGGCTAAGAG	AAGGGCATCTTTGGACTGC
mGabrb1	GCAAACAAGACCAGAGTGCC	AGGAGAATATTGCCGTGGGC
mGabrg2	ATAAGGATGCTGTTCCTGCC	GTGACATAGGAGACCTTGGGC
mGapdh	CTGCACCACCAACTGCTTAG	GTCTTCTGGGTGGCAGTGAT
mHras1	GAAACATCAGCCAAGACCCG	TCCGCAATTTATGCTGCCG
mInsr	TCTTTCTTCAGGAAGCTACATCTG	TGTCCAAGGCATAAAAAGAATAGTT
mIrs1	CTATGCCAGCATCAGCTTCC	TTGCTGAGGTCATTTAGGTCTTC
mIrs2	TCCAGAACGGCCTCAACTAT	GGCTCCAGGAGTTCTTGTCTC
mJak2	CGAGAAGAGTAAAAGTCCACCC	GGAACACAATCATTGCCCCTTG
mLepr	GACTTGCAGATGGTCACCCA	TGGGCTCAGACGTAGGATGA
mMc3r	AAAGCCCTCACCTTGATCGG	AGCACCATGGCGAAGAACAT
mMc4r	CAGTACGGATACGGATGCC	GCGAGCAAGGAGCTACAGAT
mMtor	TGGCCGTTATGTTCGATGGTC	CAGGATCTTCCCCTCAGCC
mNpy	CCAGCCCTGAGACACTGATTT	CATCACCACATGGAAGGGTCT
mPdk1	GTTGAAACGTCCCGTGCT	GCGTGATATGGGCAATCC
mPik3r1	CTTTCCTTGTCGGGAGAGC	TGACGCAATGCTTGACTTCG
mPomc	TCTGCTACAGTCGCTCAGGG	CGAGTTTGCAAGCCCGGAT
mPten	AGGCACAAGAGGCCCTAGAT	CTGACTGGGAATTGTGACTCC
mPtp1b	GCTTCTCCTACCTGGCTGTC	CACTGATCCTGCACTGACGA
mPtprj	CCGTGGACGTGTATGGGATT	TACTGGTCCTCTGTCTGCAC
mPvalb	ACAAAGACGCTTCTGGCCG	TCAGCGCCACTTAGCTTTCAG
mSocs3	TCGGTCAGTAGGTCCGAGAG	GGGAAGGCTTCTCCATCACC
mStat3	GACTGAGGTGTACCACCAAGG	AAGTTCACGTTCTTGGGGTTATTG
mTeptp	GGTGCAGGATACTGTGGAGG	ATCTGCTGCACCTTCTGAGC
mXrn1	TTATGGCTGTTGACGGTGTG	TGGCTGACCTAAAACGCCTC

Chapter 3 Results

3.1 Xrn1 whole-body knockout causes embryonic lethality

To investigate the physiological functions of Xrn1, I designed two gRNAs and ssODN targeting exons 2 and 6 of the *Xrn1* gene (Figure 3.1.A) and *Xrn1^{lox/+}* mice were generated by ssODN-mediated knock-in with CRISPR-Cas in zygotes. After I confirmed flox insertion in cis orientation, obtained *Xrn1^{lox/+}* mice were crossed with *CAG-Cre* mice to establish whole-body *Xrn1* knockout mice. *Xrn1^{+/-}* mice were viable, fertile and didn't show any obvious defects. However, whole-body *Xrn1* null mice showed embryonic lethality around E10.5 and the null embryos showed open neural tube defects in both E9.5 and E10.5 (Figure 3.1.B). Next, I examined Xrn1 protein expression in embryos by immunoblotting and confirmed knockout of Xrn1 full length protein. Surprisingly, I observed a band below full length Xrn1 in both heterozygous and homozygous knockout embryos (Figure 3.2.A). The molecular weight of the band is around 160 kDa, and Xrn1 splicing variant lacking exon2 - exon7 has a predicted molecular weight of 167 kDa although this variant was not predicted (Figure 3.2.B). The transgenic mice were designed to delete exon 2 to 6 of Xrn1 protein, but exon 7 was skipped by alternative splicing to produce truncated protein in embryos. Importantly, the truncated protein lacks important motifs such as 5'-phosphate-binding pocket and catalytic site. Thus, I conclude that Xrn1 is essential and its mRNA binding activity and exoribonuclease activity is required for the embryonic development of mice.

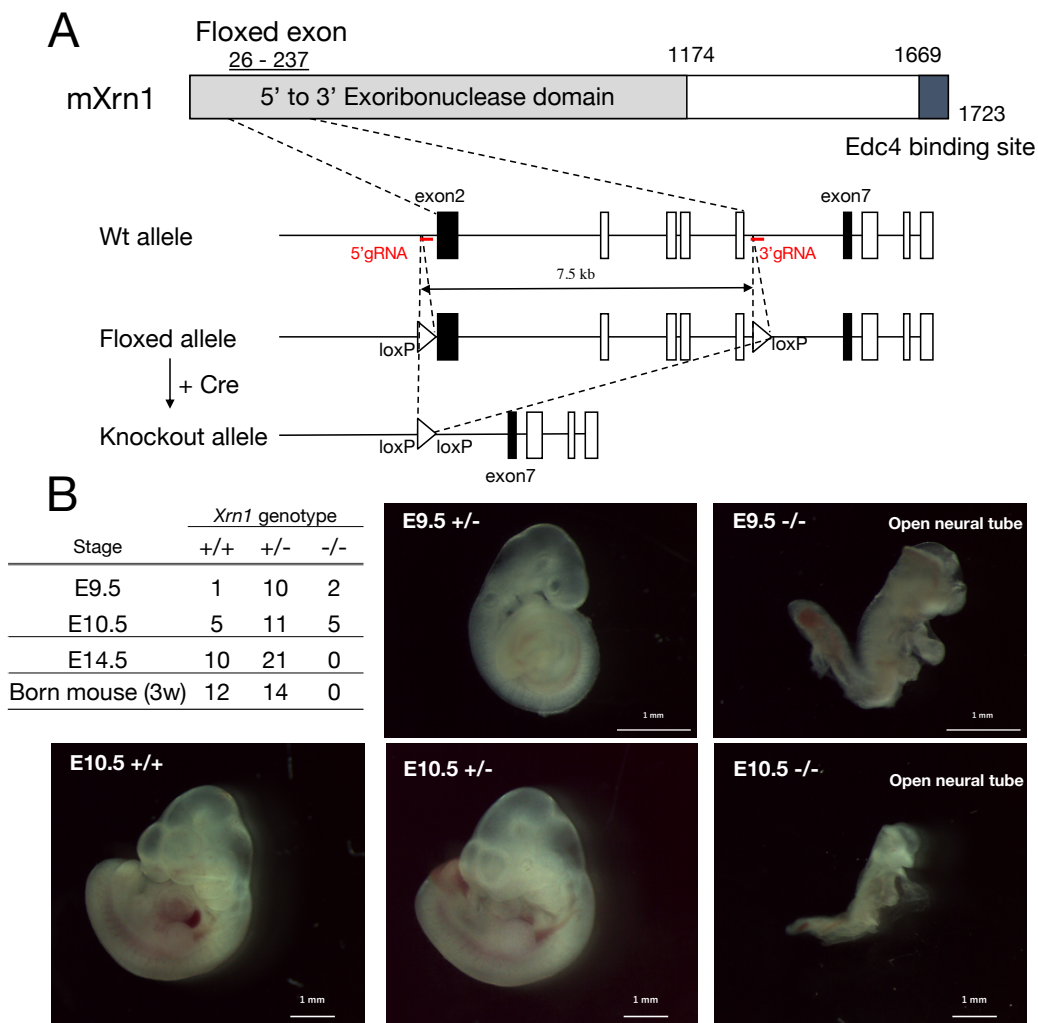


Figure 3.1| *Xrn1* knockout mice were embryonic lethal.

(A) The domain organization of mouse *Xrn1* protein and diagram of the wild-type *Xrn1* allele, the flox allele, and the knockout allele. Positions of exons, loxp sequences (white triangles), and 5' and 3' gRNAs (red line) are shown. (B) Number of embryos observed in indicated stages in each genotype. Pictures of *Xrn1*^{+/+}, *Xrn1*^{+/-}, and *Xrn1*^{-/-} embryos at indicated embryonic day.

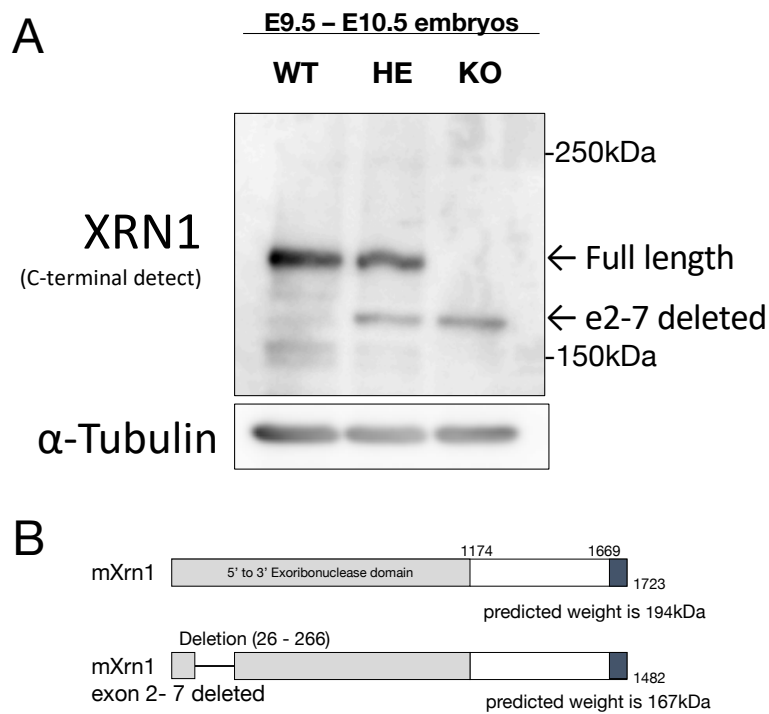


Figure 3.2| *Xrn1* knockout embryos express truncated protein.

(A) Immunoblotting for *Xrn1* and α -Tubulin in *Xrn1* WT, HE, and KO at E9.5 and E10.5 embryos. (B) Diagram of mouse *Xrn1* full length protein and truncated protein.

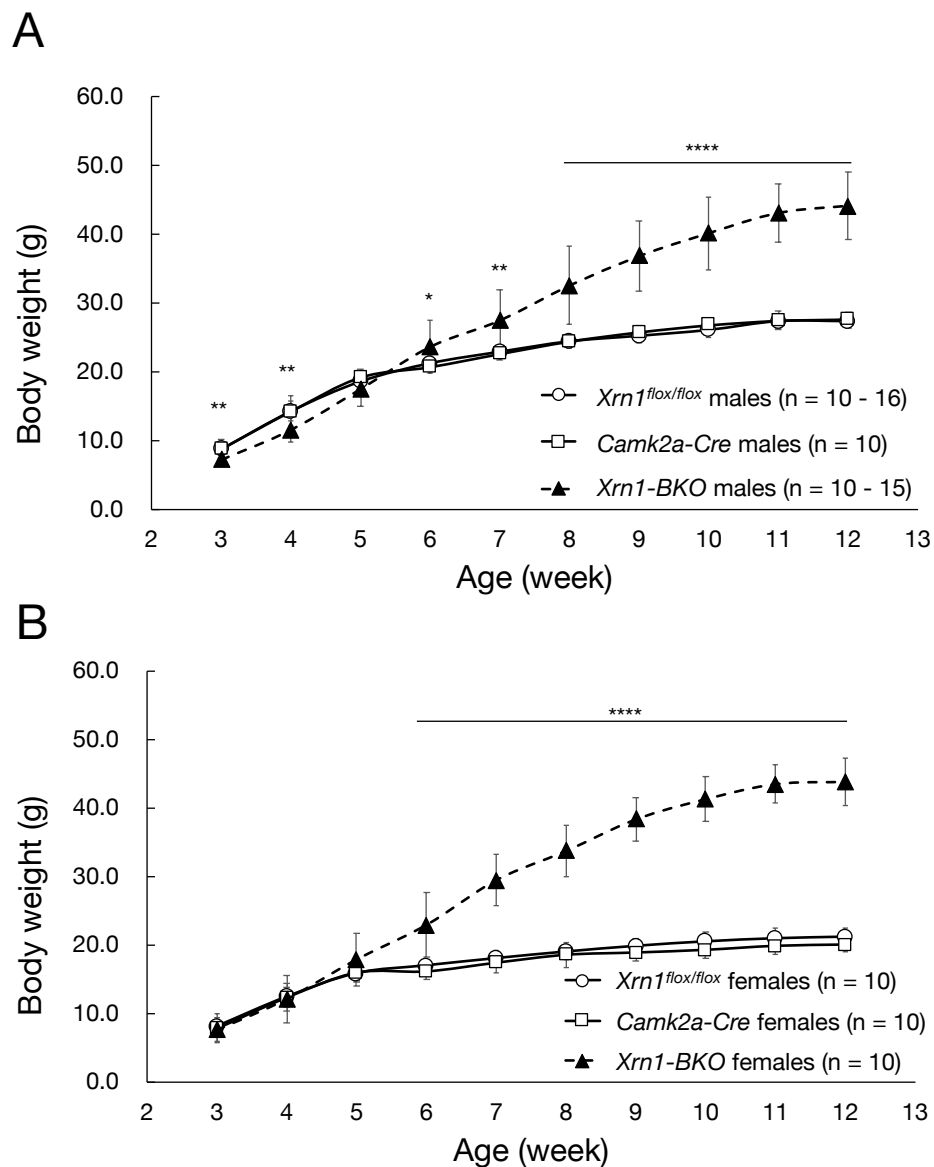


Figure 3.3| Forebrain specific *Xrn1* knockout mice were obese.

Growth curve of *Xrn1^{flox/flox}*, *Camk2a-Cre*, and *Xrn1-BKO* male (A) and female (B) mice from 3 to 12 weeks after birth. Number of mice used for the experiment is indicated in each figure. Data represents mean \pm SD. Two-Way ANOVA, * $p < 0.05$; ** $p < 0.01$; *** $p < 0.001$; and **** $p < 0.0001$.

3.2 Forebrain specific Xrn1 knockout mice were obese

Whole-body homozygous deficiency of the *Xrn1* gene was lethal in embryo (Figure 3.1). Therefore, in order to investigate physiological function of Xrn1 in adult brain, I generated forebrain specific Xrn1 knockout mice (*Xrn1-BKO*) by crossing *Xrn1^{fllox/fllox}* mice and *Camk2a-cre* mice. Surprisingly, *Xrn1-BKO* showed obesity under normal chow diet in both male and female mouse (Figure 3.3). A significant weight gain appeared at 6 weeks of age in both genders, but male mice at weaning period (3 to 4 weeks of age) were significantly smaller than control mice. Also, *Xrn1-BKO* mice had longer body length that of control littermates (Figure 3.4). Based on these results, I hypothesized that loss of Xrn1 in brain causes dysregulation in metabolism and energy homeostasis.

3.3 Xrn1-BKO mice exhibited hyperphagia, adiposity, and liver steatosis

Since I observed severe weight gain in *Xrn1-BKO* mice, next I examined daily food intake in both young period (6 – 7 weeks of age) and adult period (12 – 13 weeks of age). Mice were single-caged and daily food intake per cage under normal-chow diet was measured by calculating the difference between the initial and the remaining amount of food. There were significant differences between control mice and *Xrn1-BKO* mice in both male and female (Figure 3.5).

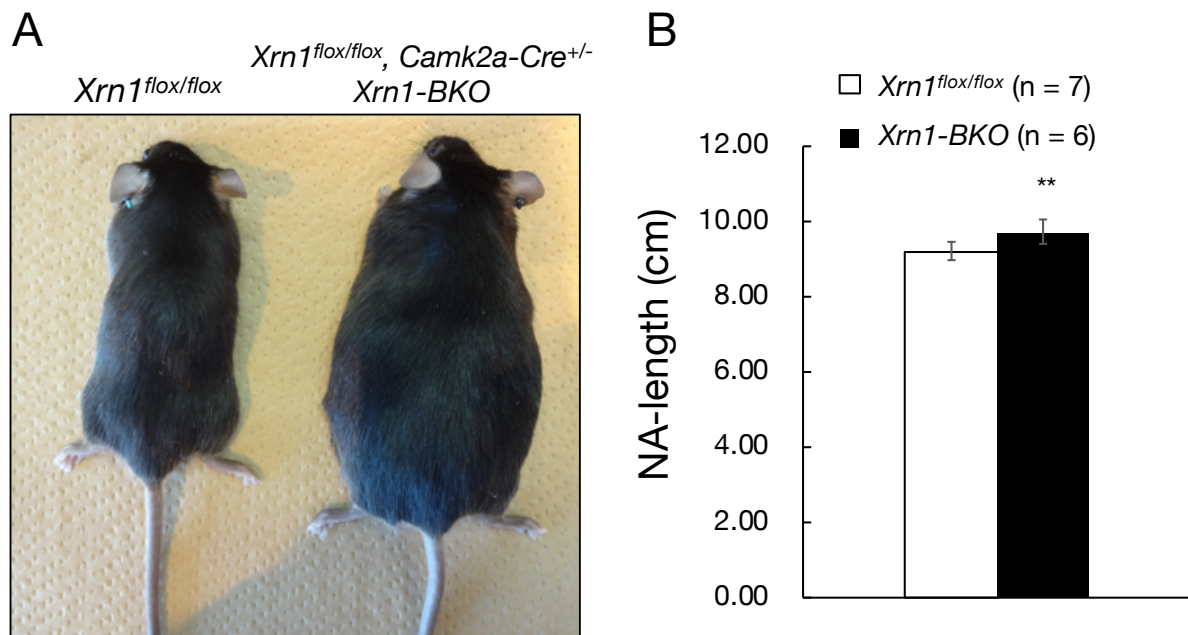


Figure 3.4| Appearance of *Xrn1* knockout mice.

(A) Picture of 13-week-old male *Xrn1^{flox/flox}* and *Xrn1-BKO* littermates. (B) Comparison of body length (right) of 12-week-old *Xrn1^{flox/flox}* and *Xrn1-BKO* mice. Data represents mean \pm SD. Unpaired t-test, * $p < 0.05$; ** $p < 0.01$; *** $p < 0.001$; and **** $p < 0.0001$.

This result clearly showed that *Xrn1-BKO* mice are hyperphagic. Next, to check whether the weight gain is actually caused by the increase in fat mass, I dissected *Xrn1-BKO* mice and control mice to compare the weight of adipose tissues and liver. In *Xrn1-BKO* mice, I observed an increase in adipose tissues weight (inguinal white adipose tissue (iWAT), epididymal white adipose tissue (eWAT), and brown adipose tissue (BAT)) and liver weight (Figure 3.6). Also, I examined the weight of brain. Interestingly, brain was smaller than control littermates (Figure 3.6), although the cause is unknown. To check the *Xrn1* knockout efficiency in brain, I examined *Xrn1* protein expression in various brain regions. I found that *Xrn1* protein is decreased in cortex, hippocampus, midbrain, and hypothalamus in *Xrn1-BKO* (Figure 3.7A). I also examined *Xrn1* protein expression in peripheral tissues. I found that *Xrn1* protein is increased in liver and thymus, but not changed in iWAT, pancreas, and muscle (Figure 3.7B). In brain and peripheral tissue lysates, I couldn't observe the truncated *Xrn1* protein expressed in whole-body *Xrn1* knockout embryos.

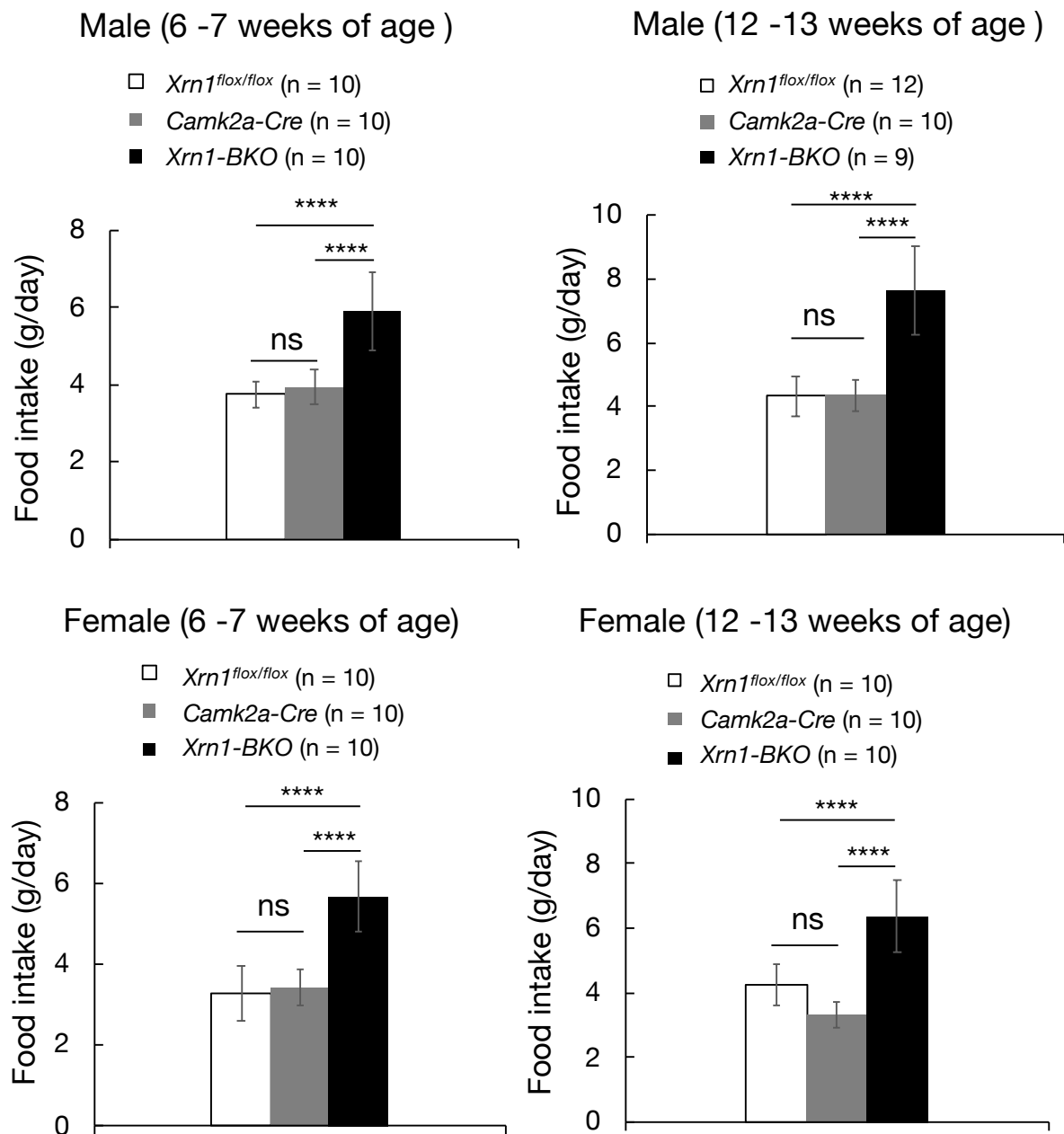
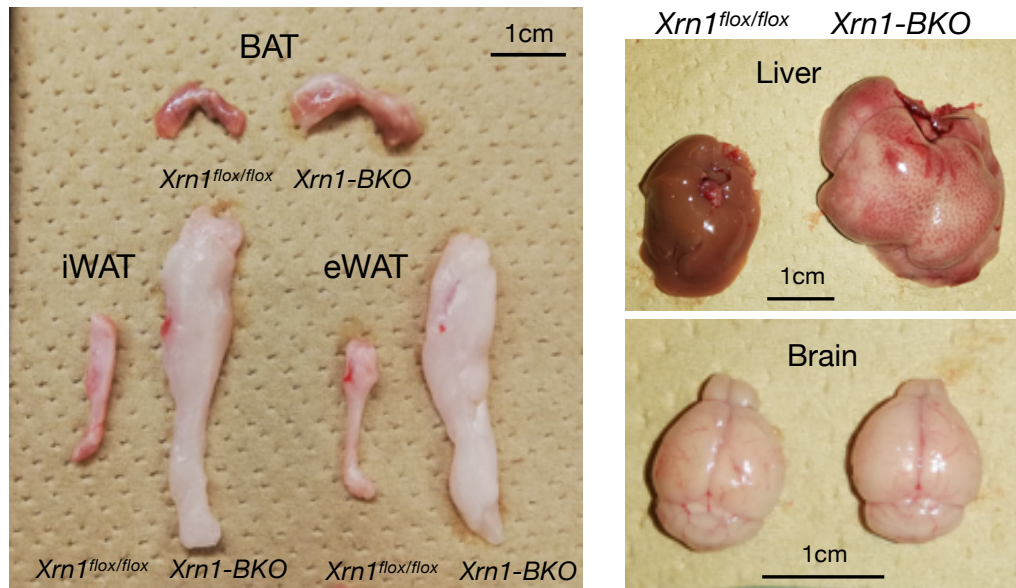


Figure 3.5| *Xrn1-BKO* mice exhibited hyperphagia.

Comparison of average daily food intake in young period and adult period of each genotype in both genders. Data represents mean \pm SD. Two-Way ANOVA, post-hoc Tukey test, * $p < 0.05$; ** $p < 0.01$; *** $p < 0.001$; and **** $p < 0.0001$.

A



B

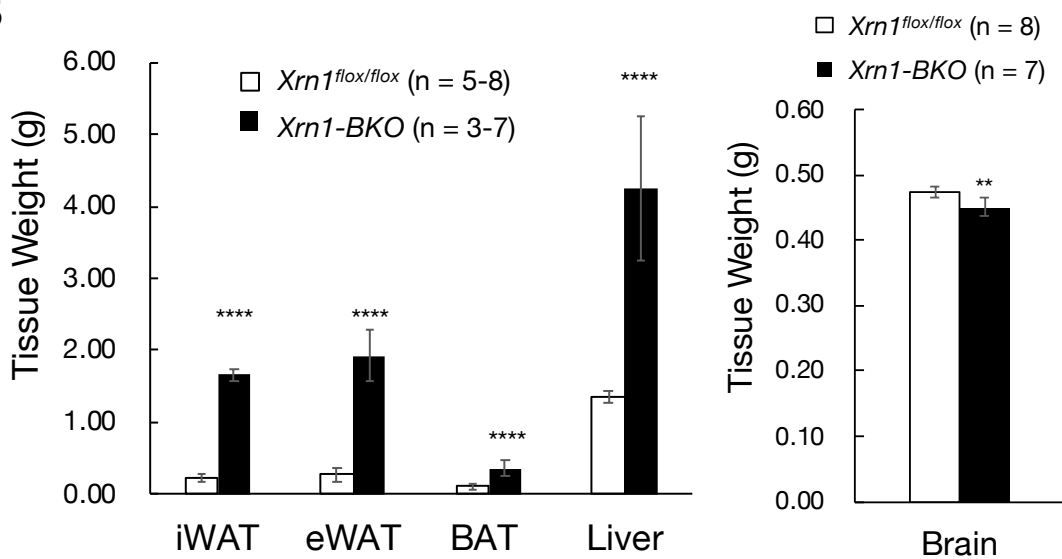


Figure 3.6| *Xrn1-BKO* mice exhibited adiposity, and liver steatosis.

(A) Gross appearance of eWAT, iWAT, BAT, Liver, and brain in 12-week-old *Xrn1^{flox/flox}* and *Xrn1-BKO* littermates. (B) Tissue weights of *Xrn1^{flox/flox}* and *Xrn1-BKO* mice at 12 weeks of age. Data represents mean \pm SD. Unpaired t-test, * $p < 0.05$; ** $p < 0.01$; *** $p < 0.001$; and **** $p < 0.0001$.

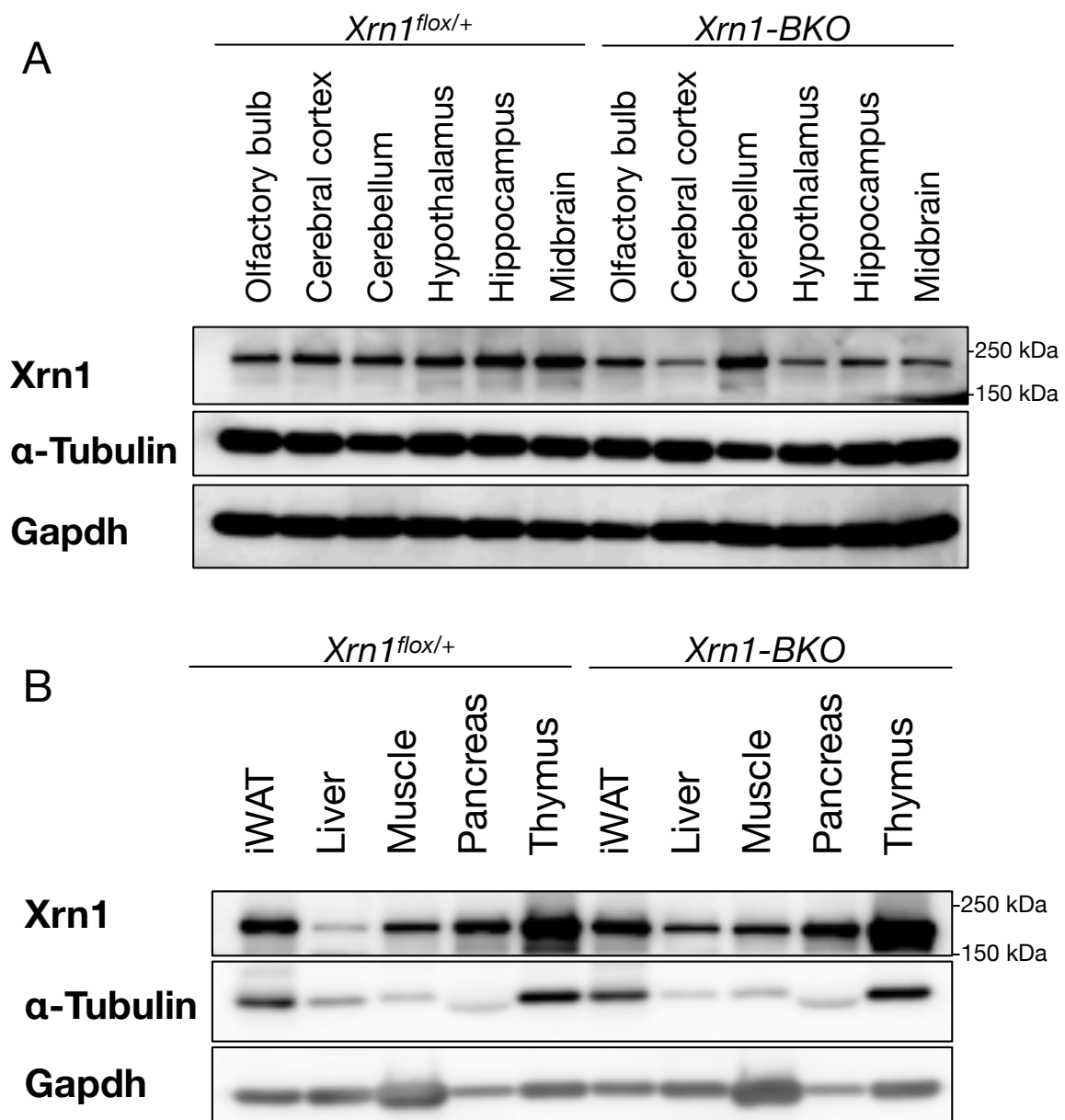


Figure 3.7| Expression of Xrn1 protein in mouse brain and peripheral tissues.

Immunoblotting for Xrn1, α-Tubulin, and Gapdh in *Xrn1-BKO* and control (*Xrn1^{flox/+}*) female mice at 12 weeks of age. (A) Lysate from brain and (B) other tissues.

3.4 *Xrn1-BKO* mice exhibited hyperglycemia, hyperleptinemia, and hyperinsulinemia

To address the relationship between increased fat masses in *Xrn1-BKO* mice and adipocyte function, I examined glucose and lipid metabolism and found that the levels of circulating blood glucose, serum leptin, and serum insulin were significantly higher in *Xrn1-BKO* mice than control mice (Figure 3.8). I also examined levels of circulating blood glucose in young period (5 – 6 weeks of age) and found that there was no significant difference, but I observed a tendency toward an increase in blood glucose level in 6 weeks of age of *Xrn1-BKO* mice. Thus, together with the body weight data, the development of obesity and diabetes like phenotypes starts around 6 weeks of age in *Xrn1-BKO* mice. In obesity and diabetes model mice, leptin resistance and insulin resistance are often observed (Balland and Cowley 2015, Huang et al. 2018).

3.5 Metabolic alteration in *Xrn1-BKO* mice

I next measured whole-body metabolism by using calorimeter and found that loss of *Xrn1* in brain resulted in a significant increase in CO₂ production (Figure 3.9A). There were no differences in O₂ consumption but increased energy expenditure (Figure 3.9B, D). Interestingly, *Xrn1-BKO* mice showed significant increase in respiratory exchange ratio (RER) (Figure 3.9C), which is calculated by VCO_2/VO_2 . RER is the indicator of energy source. If carbohydrates are only used as the energy source, RER becomes 1.0. On the other hands, if fat is solely used as the energy source, RER will be 0.7. In control mice, RER is oscillating during a day, however, *Xrn1-BKO* mice showed constant RER and the value is about 1.0. These results indicate that

lack of *Xrn1* in brain altered whole-body energy substrate utilization. I also measured activity of mice using home cage activity monitoring system and I didn't observe significant difference although there was a decrease in activity during light period in *Xrn1-BKO* mice (Figure 3.10). The variance in control mice were huge in this experiment, thus further investigation of *Xrn1-BKO* activity is required.

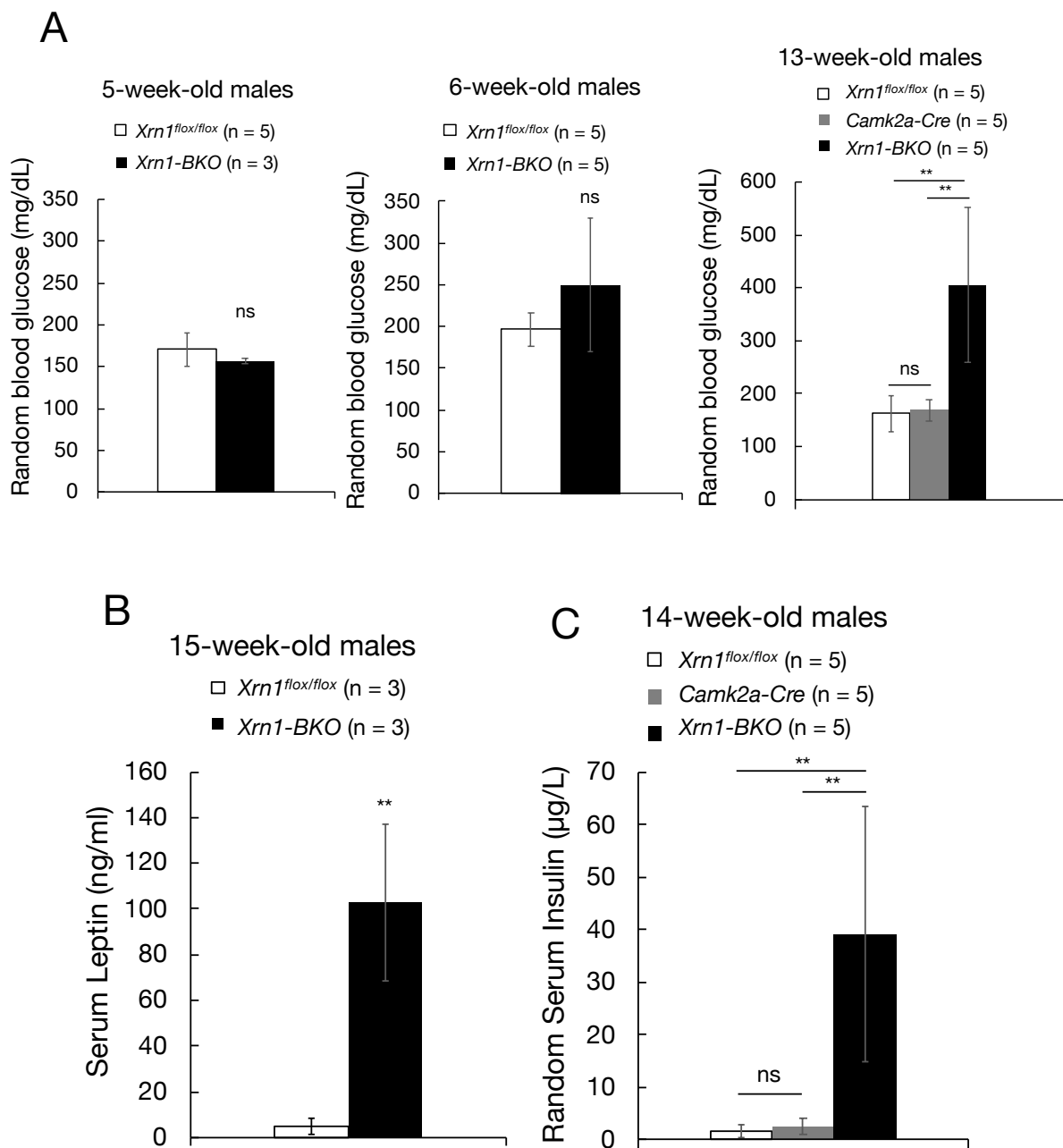


Figure 3.8| *Xrn1-BKO* mice exhibited hyperglycemia, hyperleptinemia, and hyperinsulinemia.

(A) Levels of circulating random blood glucose in each age. (B-C) Levels of circulating serum leptin (B) and insulin (C) concentration measured by ELISA. Data represents mean \pm SD. Unpaired t-test (two sample groups). Two-Way ANOVA, post-hoc Tukey test (three sample groups), * $p < 0.05$; ** $p < 0.01$; *** $p < 0.001$; and **** $p < 0.0001$.

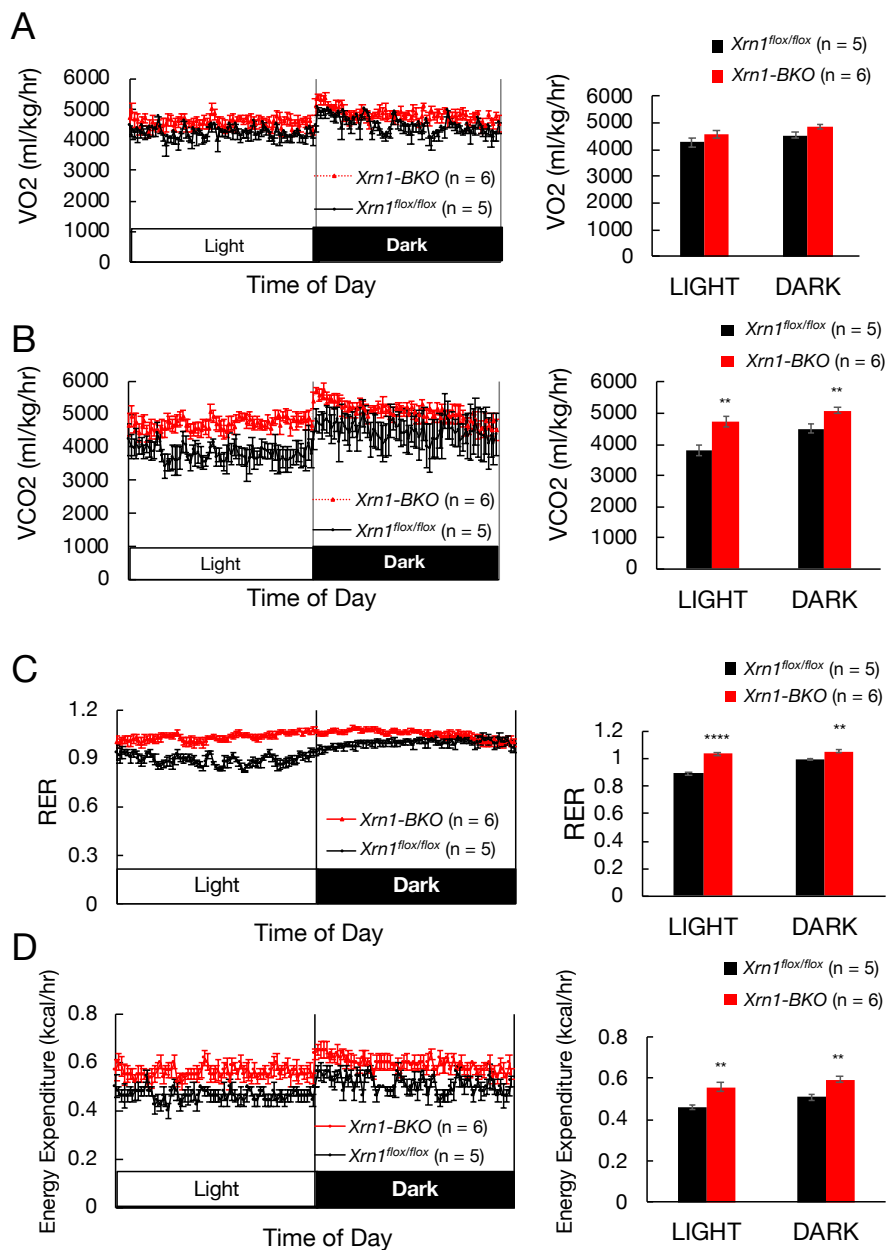


Figure 3.9| *Xrn1*-BKO mice displayed increased VCO₂, energy expenditure, and constant RER.

(A) Oxygen consumption, (B) carbon dioxide production, (C) respiratory exchange ratio (RER), and (D) energy expenditure of 6 to 7-week-old mice were measured. RER is calculated by VCO₂ divided by VO₂. RER equals to 1.0 means carbohydrate is dominant energy source. RER equals to 0.7 means fat is dominant energy source. Data represents mean ± SEM. Unpaired t-test, **p*<0.05; ***p*<0.01; ****p*<0.001; and *****p*<0.0001.

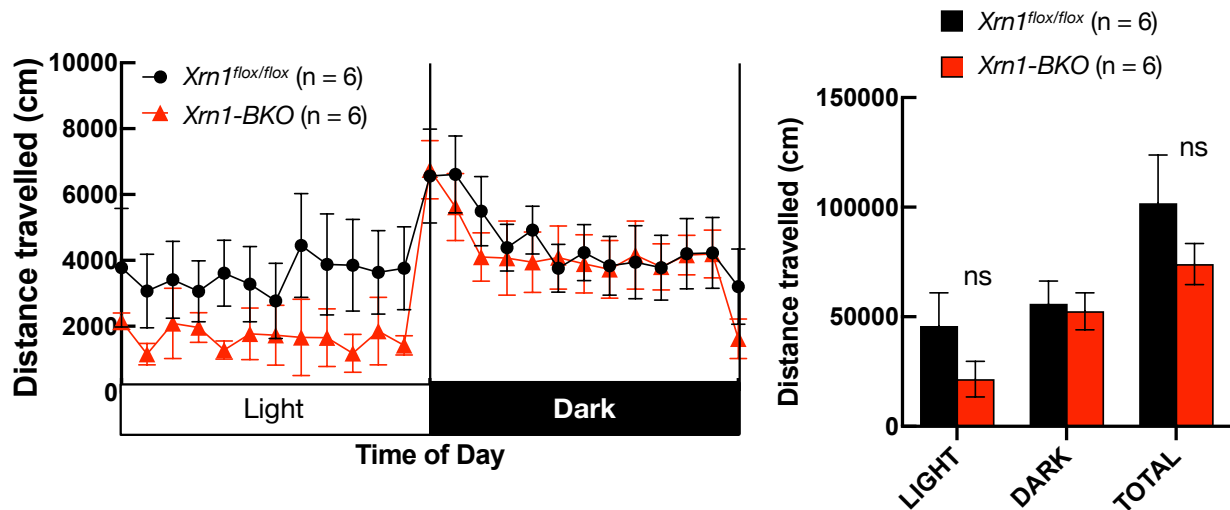


Figure 3.10| *Xrn1-BKO* mice didn't show statistical changes in activity.

(A) Home cage activity monitoring of 6 to 8-week-old male mice. Data represents mean \pm SEM. Unpaired t-test, * $p < 0.05$; ** $p < 0.01$; *** $p < 0.001$; and **** $p < 0.0001$.

3.6 *Xrn1-BKO* mice exhibited upregulation of appetite and energy homeostasis related genes in hypothalamus

The above data suggest that *Xrn1-BKO* mice had a defect in appetite and energy homeostasis control. The hypothalamus controls energy homeostasis by receiving and integrating metabolite signals such as hormones and blood glucose levels from the peripheral tissues including liver, pancreas, and adipose tissue (St-Pierre and Tremblay 2012). A well-known neural circuit that controlling appetite and energy homeostasis in hypothalamus is the melanocortin system. In the arcuate nucleus of the hypothalamus (ARC), anorexigenic proopiomelanocortin (POMC) expressing neurons and orexigenic agouti-related protein (AgRP) expressing neurons exist. Both neurons are projecting to the paraventricular nucleus of the hypothalamic (PVH) and

dorsomedial nucleus of the hypothalamus (DMH) where melanocortin receptor expressing neurons are present. POMC is a precursor of α -melanocyte stimulating hormone (α -MSH), and α -MSH is a ligand of melanocortin receptors, MC3R and MC4R (Pritchard, Turnbull, and White 2002). Upregulation of melanocortin receptor signaling in hypothalamus causes satiety. AgRP is an antagonist of the melanocortin receptor signaling pathway, thus overexpression of AgRP leads to hyperphagia and obesity (Graham et al. 1997, Ollmann et al. 1997). Activity of both POMC and AgRP neurons are regulated by hormones such as leptin and insulin, and also by nutrients such as glucose via JAK-STAT signaling pathways and PI3K-AKT signaling pathways (Belgardt, Okamura, and Brüning 2009, Wunderlich, Hövelmeyer, and Wunderlich 2013, Huang et al. 2018)

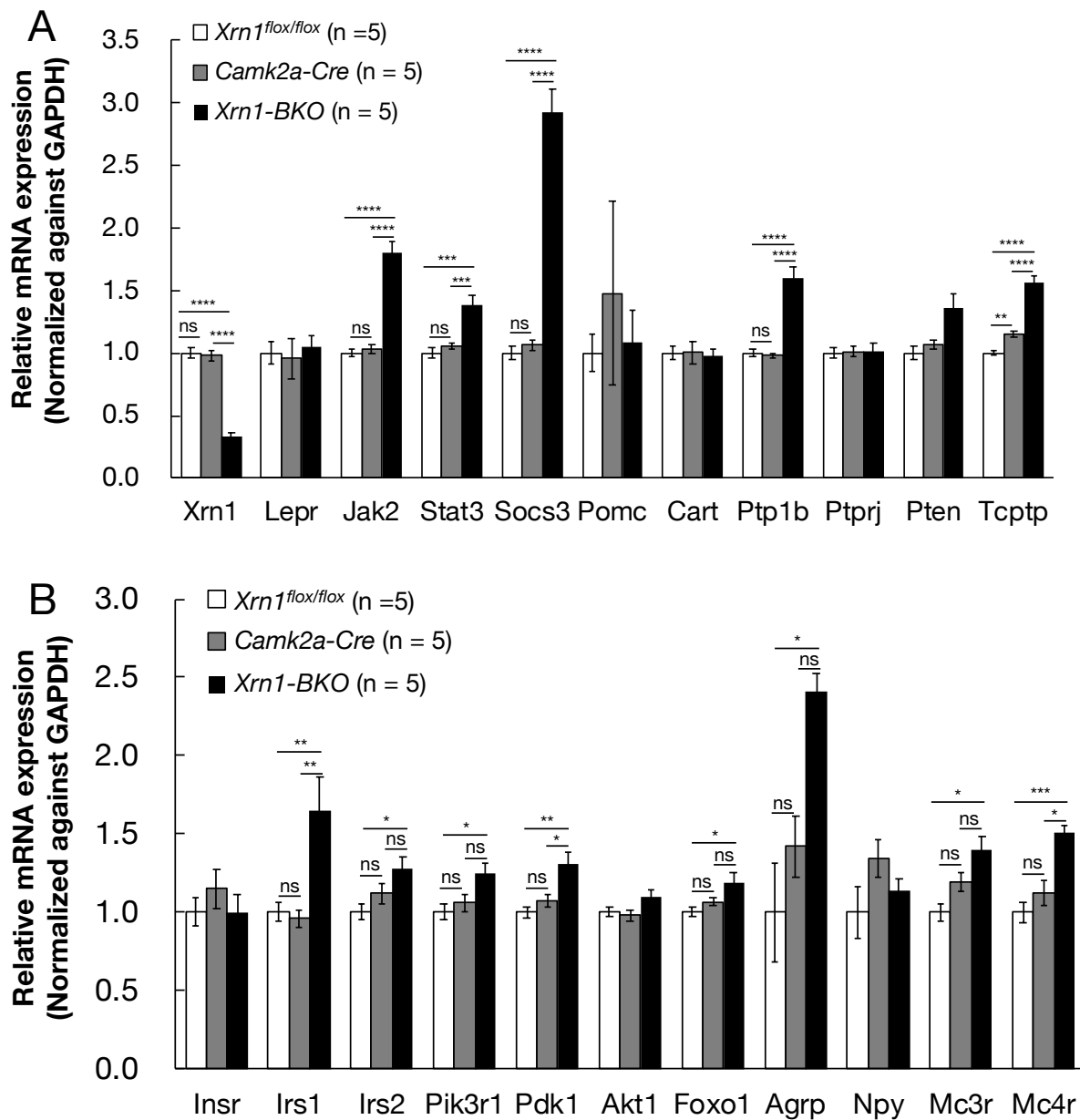


Figure 3.11| *Xrn1-BKO* mice exhibited upregulation of appetite and energy homeostasis related genes in hypothalamus.

Quantitative PCR analysis of the indicated mRNA levels in hypothalamus of 10 to 14-week-old male mice. Data represents geometric mean \pm SEM. Two-Way ANOVA, post-hoc Tukey test, * $p < 0.05$; ** $p < 0.01$; *** $p < 0.001$; and **** $p < 0.0001$.

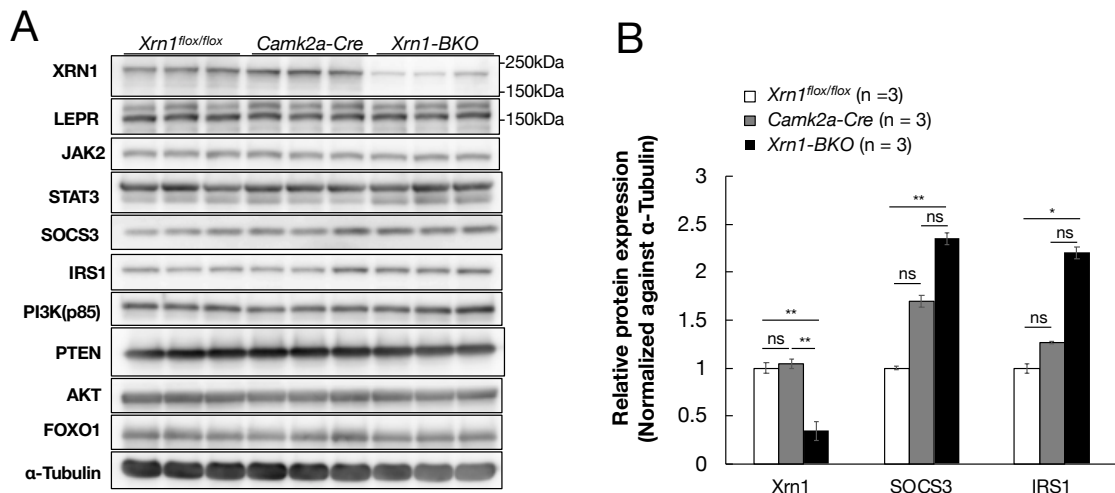


Figure 3.12| Leptin and insulin signaling related protein expression in *Xrn1-BKO* mice hypothalamus.

(A) Immunoblot of hypothalamus lysate from 12 to 14-week-old male mice. (B) Protein quantification of subunits normalized relative to α -tubulin levels. WT values were normalized to 1. Data represents mean \pm SEM. Two-Way ANOVA, post-hoc Tukey test, * $p < 0.05$; ** $p < 0.01$; *** $p < 0.001$; and **** $p < 0.0001$.

Based on the above fact, I performed quantitative real-time PCR (qPCR) analysis in hypothalamus and found that the levels of mRNAs relevant to appetite and energy homeostasis were increased in hypothalamus of *Xrn1-BKO* mice. Those included mRNAs encoding AgRP and inhibitors of Jak-Stat and PI3K-Akt signaling pathway, *Socs3*, *Ptp1b*, and *Tcptp* (Figure 3.11). Next, I performed immunoblotting to check protein expression in hypothalamus and found that *Socs3* and *Irs1* were upregulated in *Xrn1-BKO* mice (Figure 3.12). Moreover, I also observed increased AgRP protein expression and decreased *Pomc* expression in ARC in *Xrn1-BKO* mice by immunohistochemistry (Figure 3.13).

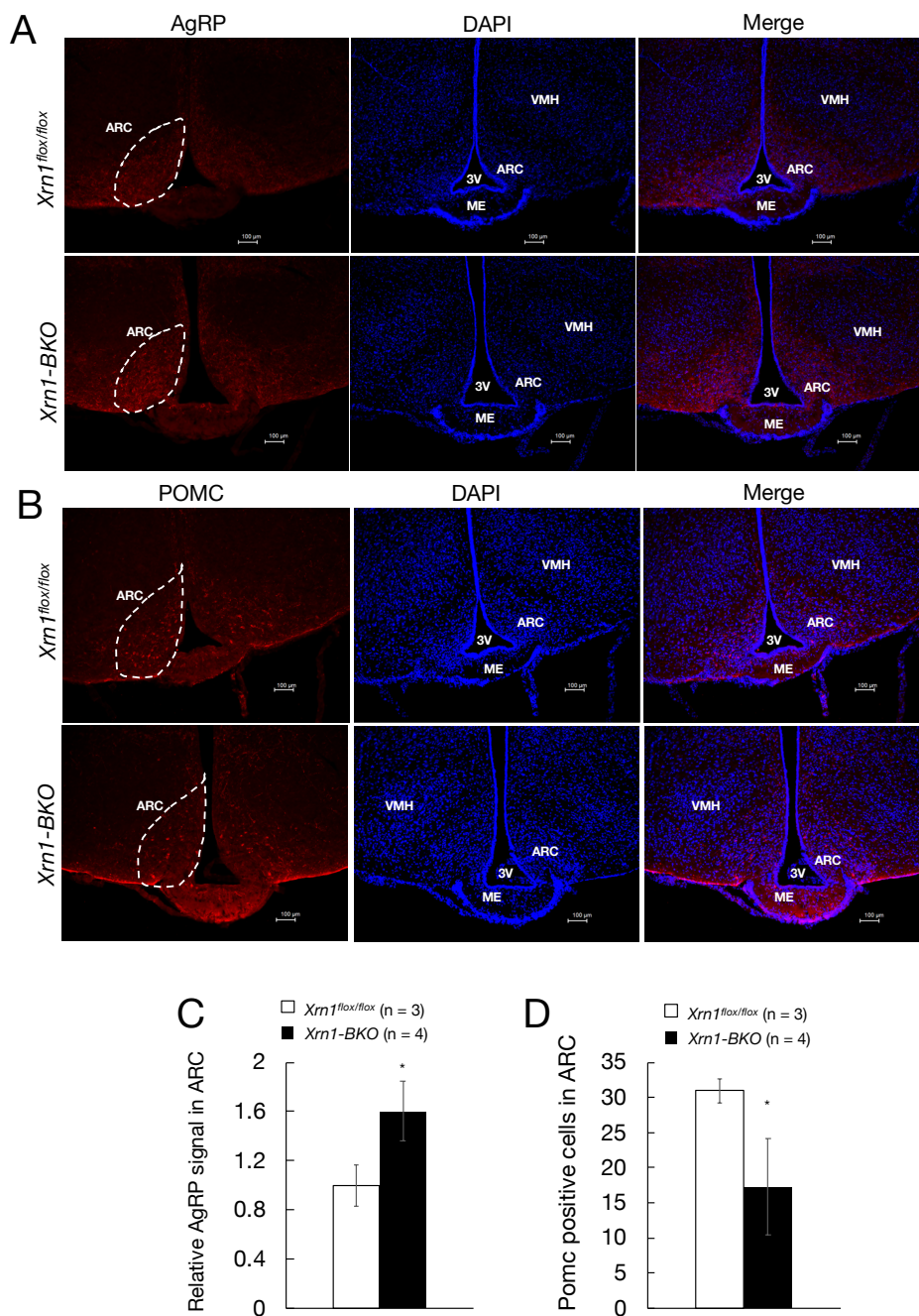


Figure 3.13| *Xrn1-BKO* mice displayed increased AgRP expression and decreased Pomc expression in hypothalamus.

(A) Immunostaining for AgRP (red) and counterstained with DAPI (blue) in *Xrn1-BKO* and control (*Xrn1^{flox/flox}*) mice at 12 weeks of age (B) Immunostaining for Pomc (red) and counterstained with DAPI (blue) in *Xrn1-BKO* and control (*Xrn1^{flox/flox}*) mice at 12 weeks of age. (C, D) Quantification of AgRP staining and Pomc staining. Data represents mean \pm SEM. Unpaired t-test, * $p < 0.05$; ** $p < 0.01$; *** $p < 0.001$; and **** $p < 0.0001$.

3.6 Proteomics analysis in *Xrn1-BKO* hypothalamus

To investigate the relationships between protein expression and observed abnormalities in *Xrn1-BKO* mice, I performed comprehensive proteomics analysis using Mass spectrometer. I could identify 3632 proteins by Mass spec. In hypothalamus of *Xrn1-BKO* mice, 44 proteins significantly increased more than 1.5-fold compared to those of control mice. Conversely, 76 proteins in *Xrn1-BKO* hypothalamus significantly decreased more than 1.5-fold (Figure 3.14).

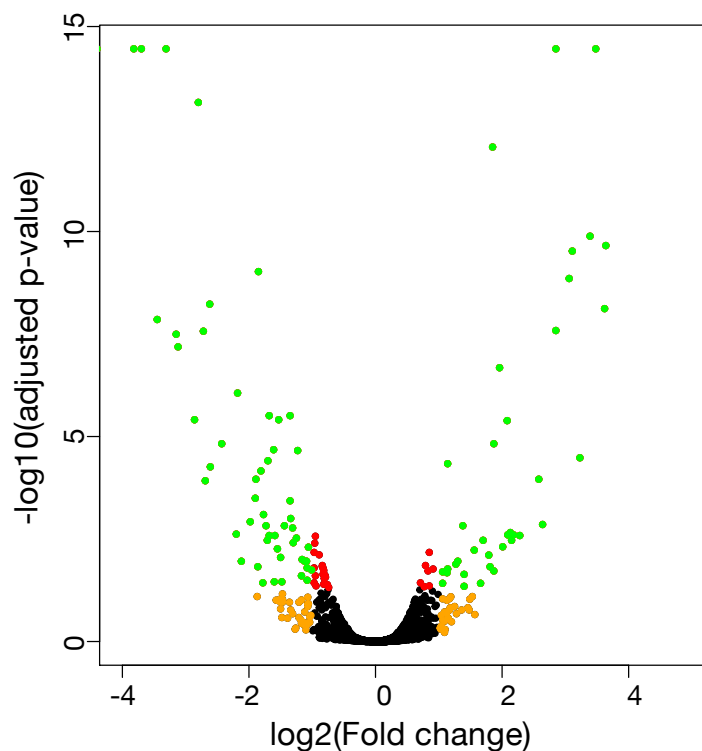


Figure 3.14| Volcano plot from the proteomics analysis in hypothalamus.

Volcano plot showing log₂ fold change (BKO/control) and adjusted p-values. Red dots represent proteins having significant adjusted p-values (adj. p-value < 0.05), yellow dots represent proteins having fold-change larger than 2 but not significant. Green dots represent proteins having fold-change larger than 2 and significant adjusted p-values.

Table 3.1| Differentially expressed proteins related to metabolism and hormone signaling.

Gene name	Description	log2 Fold Change	Adj. P-Value
Vldlr	Very low-density lipoprotein receptor	3.64	2.2E-10
Aldob	Fructose-bisphosphate aldolase B	2.18	2.5E-03
Ephx2	Bifunctional epoxide hydrolase 2	2.13	2.2E-03
Cyth3	Cytohesin-3	2.09	2.5E-03
Mcat	Malonyl-CoA-acyl carrier protein transacylase	2.08	4.1E-06
Nsg1	Neuronal vesicle trafficking-associated protein 1	1.81	1.5E-02
Mtor	Serine/threonine-protein kinase mTOR	1.3	1.1E-02
Apoe	Apolipoprotein E	0.85	6.7E-03
Fabp3	Fatty acid-binding protein, heart	0.71	3.7E-02
Flot1	Flotillin-1	-0.79	2.7E-02
Flot2	Flotillin-2	-0.8	2.5E-02
Acot7	Cytosolic acyl coenzyme A thioester hydrolase	-0.89	7.7E-03
Acacb	Acetyl-CoA carboxylase 2	-0.95	2.7E-03
Vamp2	Vesicle-associated membrane protein 2	-0.96	4.0E-03
Hras1	GTPase HRas	-1.09	1.1E-02
Atp6v1f	V-type proton ATPase subunit F	-1.34	1.0E-03
Akt3	RAC-gamma serine/threonine-protein kinase	-1.89	1.1E-04

Table 3.2| Differentially expressed proteins related to brain.

Gene name	Description	log2 Fold Change	Adj. P-Value
Cacnb3	Voltage-dependent L-type calcium channel subunit beta-3	3.23	3.3E-05
Gabrg2	Gamma-aminobutyric acid receptor subunit gamma-2	1.87	1.5E-05
Pvalb	Parvalbumin alpha	0.91	1.7E-02
Gls	Glutaminase kidney isoform, mitochondrial	-0.76	4.1E-02
Sytl4	Synaptotagmin-like protein 4	-0.82	1.9E-02
Cnrip1	CB1 cannabinoid receptor-interacting protein 1	-0.82	4.0E-02
Gabbr1	Gamma-aminobutyric acid receptor subunit beta-1	-1.3	3.9E-03
Cox7a2	Cytochrome c oxidase subunit 7A2, mitochondrial	-1.35	3.7E-04
Ngb	Neuroglobin 1	-1.44	1.5E-03
Th	Tyrosine 3-monooxygenase	-1.86	1.5E-02
Astn2	Astrotactin-2	-3.82	3.5E-15

Table 3.3| Differentially expressed proteins related to mRNA metabolism.

Gene name	Description	log2 Fold Change	Adj. P-Value
Lsm14b	Protein LSM14 homolog B	3.48	3.5E-15
Poldip3	Polymerase delta-interacting protein 3	2.58	1.1E-04
Ddx6	Probable ATP-dependent RNA helicase DDX6	1.85	8.7E-13
Ybx1	Nuclease-sensitive element-binding protein 1	1.79	7.8E-03
Celf2	CUGBP Elav-like family member 2	0.83	1.9E-02
Sf3b3	Splicing factor 3B subunit 3	-0.94	4.4E-02
Rpl22	60S ribosomal protein L22	-1.01	1.8E-02
Rnmt	mRNA cap guanine-N7 methyltransferase	-1.08	1.6E-02
Hnrnp2	Heterogeneous nuclear ribonucleoprotein H2	-1.53	3.9E-06
Csad	Cysteine sulfinic acid decarboxylase	-1.81	6.9E-05
Dkc1	H/ACA ribonucleoprotein complex subunit DKC1	-2.2	2.4E-03

To characterize protein expression differences in hypothalamus, I created the lists of the upregulated and downregulated proteins in different biological process (Table 3.1-3). Mammalian or mechanistic target of rapamycin (mTOR) senses and integrates various signals and regulates many cellular and physiological processes including energy homeostasis in hypothalamus by controlling through a PI3K/Akt-mediated pathway (Hu, Xu, and Liu 2016). Also, it is known that gamma-Aminobutyric acid (GABA) has a major role in feeding (Horvath et al. 1997) . AgRP neurons produce GABA and inhibit POMC neurons by GABAergic-mediated inhibition (Cowley et al. 2001, Tong et al. 2008).

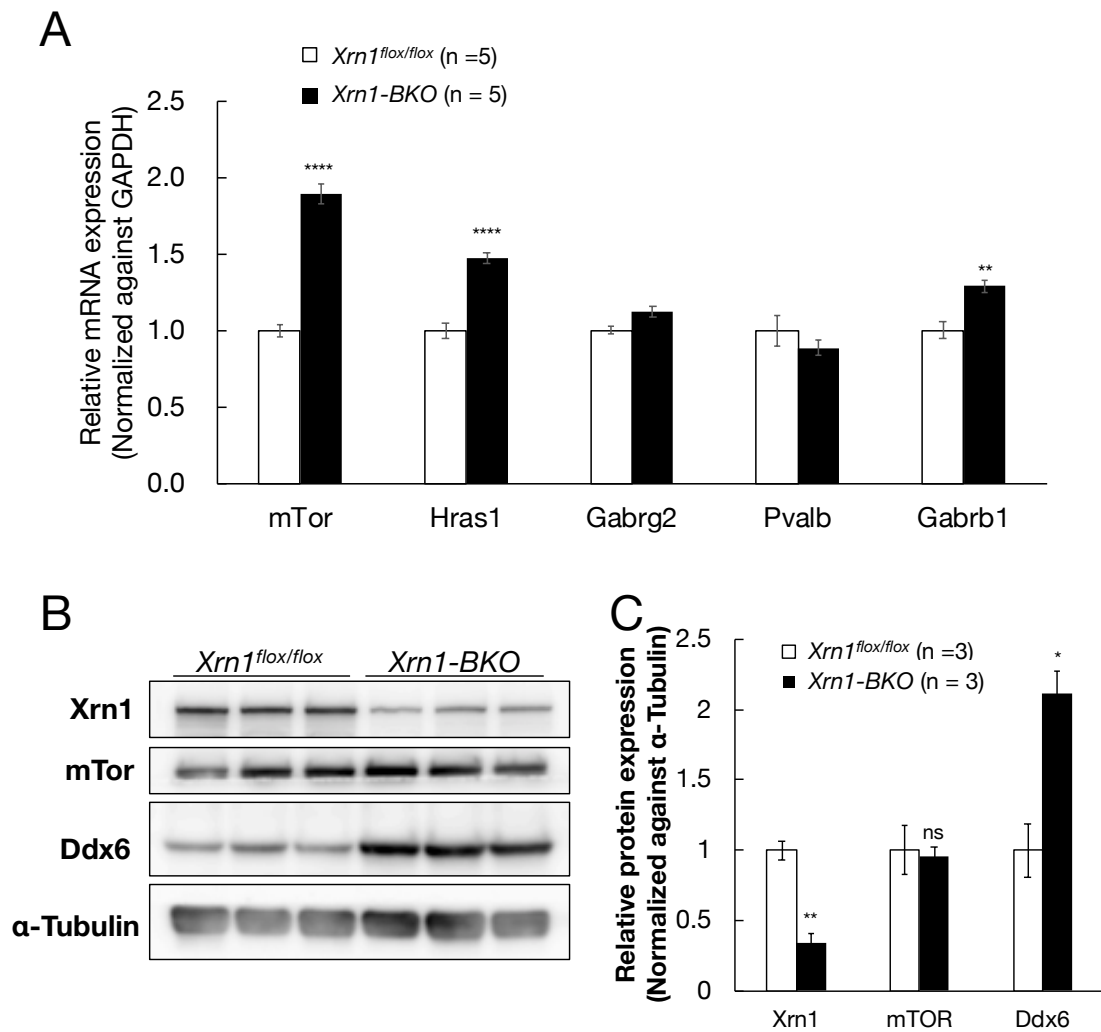


Figure 3.15 | Validation of the result of the proteomics analysis by qPCR and immunoblotting.

(A) qPCR analysis of the indicated mRNA levels in hypothalamus of 10 to 14-week-old male mice. (B) Immunoblotting of hypothalamus lysate from 11-week-old male mice. (C) Protein quantification of indicated proteins. Data represents geometric mean \pm SEM. Unpaired t-test, * $p < 0.05$; ** $p < 0.01$; *** $p < 0.001$; and **** $p < 0.0001$.

Therefore, I examined mRNA expression of mTor and GABA receptors by qPCR analysis (Figure 3.15A). The result showed that mTor mRNA was significantly increased in *Xrn1-BKO* hypothalamus. On the other hand, GABA receptor *Gabrg2* was not changed and *Gabrb1* was slightly increased although *Gabrb1* was screened as downregulated protein in mass spec analysis (Figure 3.15A). To confirm protein upregulation of mTor, I performed immunoblotting by using the same lysate that I used in proteomics analysis. Unfortunately, I couldn't validate the upregulation of mTor by immunoblotting (Figure 3.15B). However, upregulation of *Ddx6*, which is an RNA helicase, was validated. Thus, further investigation of the result of proteomics analysis is required.

Chapter 4 Discussion

4.1 Functions of Xrn1 in embryo genesis

The aim of my thesis study was to establish Xrn1 knockout mice for the first time and to analyze its phenotypes. In the first part of my thesis, I have shown that mice homozygously knockout for Xrn1, a gene encoding a major 5' - 3' exoribonuclease, are embryonic lethal and show open neural tube defects during embryogenesis (Figure 3.1). This result is consistent with the studies in different model organisms. RNAi mediated *xrn1* knockdown in *C. elegans* embryos leads to failure of ventral enclosure (Newbury and Woollard 2004). *Drosophila* having mutation in *PACMAN (XRNI)* show developmental defects including a cleft thorax phenotype (Grima et al. 2008). The epithelial sheet movement and enclosure are required to fulfill embryo development and wound healing. Ventral enclosure in *C. elegans*, dorsal/thorax closure in *Drosophila*, and neural tube closure in higher vertebrate have been shown to be a similar morphological process (Jacinto, Martinez-Arias, and Martin 2001, Jacinto, Woolner, and Martin 2002). Therefore, my data provide the evidence that the function of Xrn1 in epithelial fusion is also conserved in rodents, although the key target mRNAs behind the mechanisms are still unknown. The cleft thorax phenotype observed in *PACMAN (XRNI)* mutant flies is similar to that of the flies having mutation in c-Jun N-terminal kinase (JNK) signal pathway (Agnès, Magali, and Noselli 1999). Also, loss of function mutation in both JNK1/JNK2 causes neural tube defects in mice (Sabapathy et al. 1999). Thus, it is possible that Xrn1 influences epithelial sealing mechanism by regulating JNK signaling pathway.

4.2 Xrn1 controls energy homeostasis in hypothalamus

The global epidemic of obesity and diabetes is drawing attention as a social problem. The development of these diseases is caused by numerous biological processes. Therefore, many obesity model mice have been established and analyzed to expand our understanding (Yazdi, Clee, and Meyre 2015). The first obesity model mice were discovered in 1950 (Ingalls, Dickie, and Snell 1950). The gene responsible for the mutation is called *ob*. The *ob/ob* mice show hyperphagia, hyperinsulinemia, and hyperglycemia (Coleman and Hummel 1973). More than 40 years later, the *ob* gene was cloned and identified as an adipocyte derived peptide hormone, leptin (Zhang et al. 1994, Kanasaki and Koya 2011). Another mutant mouse line that develops severe obesity was reported in 1967. This mutation was named *db*, and *db/db* mice also exhibit persistent hyperphagia and obesity, resulting in hyperglycemia, hyperinsulinemia, and hyperleptinemia (Coleman and Hummel 1967). The *db* gene was cloned and identified as a receptor of leptin (Chen et al. 1996). In recent decades, it becomes more evident that genetic defects in the leptin signaling pathway are associated with the development of obesity and diabetes (Yazdi, Clee, and Meyre 2015). In my thesis study, I provide evidence that forebrain specific knockout of the 5'-3' exoribonuclease *Xrn1* causes obesity. Also, these mice exhibit hyperphagia, resulting in hyperglycemia, hyperinsulinemia, and hyperleptinemia. I further showed that leptin signaling related gene expressions are altered in the hypothalamus of *Xrn1*-*BKO* mice.

In obesity model mice, hyperleptinemia is often observed. In normal conditions, increased adiposity leads to more leptin production. An increase in circulating leptin levels is

detected by the hypothalamus and causes metabolic shifts to maintain energy homeostasis. However, obese individuals are less sensitive to leptin. Thus, they are resistant to leptin's anorexigenic effect. This phenomenon is called "leptin resistance" (St-Pierre and Tremblay 2012). Previous studies have shown that leptin resistance is caused by various mechanisms such as endoplasmic reticulum (ER) stress, inflammation, and attenuation of leptin signaling by SOCS3 and protein tyrosine phosphatases (Björbæk et al. 1998, Zhang et al. 2008, White et al. 2009, Loh et al. 2011, St-Pierre and Tremblay 2012, Tanti et al. 2013). I showed that *Xrn1-BKO* mice are obese and their serum leptin levels are high (Figure 3.3 and 3.8). Also, *Socs3*, *Ptp1b*, and *Tcptp* mRNA were upregulated in *Xrn1-BKO* hypothalamus (Figure 3.11-12). These results indicate that *Xrn1-BKO* mice developed leptin resistance. However, upregulation of leptin resistance genes might be the consequence of obesity, rather than the cause of it. For example, *Socs3* overexpression in leptin receptor neurons does not lead to obesity but rather a lean phenotype (Reed et al. 2010). In addition, AgRP neuron specific *Socs3* overexpression doesn't cause obesity, but show the phenotype similar to that of observed in short-term consumption of a high-fat diet (Olofsson et al. 2013). *Pomc* neuron-specific *Socs3* overexpression causes obesity, but the weight gain is not severe and they are not hyperphagic (Reed et al. 2010). Therefore, the upregulation of leptin resistance-related genes is less likely to be the primary effect of loss of *Xrn1* in the brain.

Xrn1-BKO mice are not only obese but also their body was longer than that of littermates (Figure 3.4). Interestingly, *ob/ob* and *db/db* mice don't show an increase in body

length, rather they are shorter than their littermates (Dubuc 1976, Graham et al. 1997). On the other hands, AgRP overexpression mutant mice, Pomc knockout mice, Mc4r knockout mice, and MC4R deficiency human patients have longer body length (Huszar et al. 1997, Ollmann et al. 1997, Graham et al. 1997, Yaswen et al. 1999, Farooqi et al. 2003). It indicates that the phenotypes observed in *Xrn1-BKO* mice are related to the defects in the melanocortin receptor signaling pathway. *Xrn1-BKO* mice exhibit constant RER, indicating a metabolic shift of energy source (Figure 3.9C). A recent study has shown that activation of AgRP neurons alters whole-body substrate utilization (Cavalcanti-de-Albuquerque et al. 2019). In this paper, the authors showed that AgRP neuron regulates lipogenesis and glycolysis in white adipose tissue via sympathetic signaling. In consequence, activation of AgRP neurons leads to a shift in RER. AgRP mRNA and protein expressions are elevated in the hypothalamus of *Xrn1-BKO* mice (Figure 3.11 and 3.13). Based on the above fact, AgRP might be a primary target of *Xrn1* in the hypothalamus, as observed phenotypes are consistent with known AgRP overexpression mice. Although further investigations in peripheral tissues are required to conclude that metabolic alteration of *Xrn1-BKO* is due to dysregulation of lipogenesis and glycolysis. Previous studies have shown that *Xrn1* regulates its target gene expression by controlling mRNA stability, transcription, and translation (Braun and Young 2014, Luchelli, Thomas, and Boccaccio 2015). Therefore, further comprehensive analyses are required to fully clarify the mechanisms of the upregulation of AgRP in *Xrn1-BKO*. It is also worth mentioning that we must keep in mind that this mouse model is forebrain specific conditional knockout. Consideration should be given to

the possibility that loss of Xrn1 affects other brain regions such as cortex and hippocampus since I observed a reduction of Xrn1 protein in these regions (Figure 3.7).

Proteomics analysis has shown that more than 100 proteins are either upregulated or down regulated in *Xrn1-BKO* hypothalamus (Figure 3.14). The main purpose of this approach was to screen for novel potential Xrn1 target genes and proteins related to the observed phenotypes although I could only validate the upregulation of Ddx6 protein so far (Figure 3.15B). DEAD box RNA helicase Ddx6 is a homologue of yeast Dhh1 and the major activator of the decapping enzyme Dcp1. Since decapping is coupled with subsequent 5' to 3' decay, Ddx6 is an indirect activator of Xrn1 (Fischer and Weis 2002). Ddx6 is one of the core components of P-bodies (Sheth and Parker 2003, Cougot, Babajko, and Séraphin 2004, Parker and Sheth 2007). It is worth mentioning that overexpression of Ddx6 leads to an increase in p-bodies number and suppress translation in yeast (Coller et al. 2001). In *Drosophila* testis and eggs, Xrn1 is colocalized with Ddx6 in p-bodies (Zabolotskaya et al. 2008, Lin et al. 2008). Hypomorphic mutations in Xrn1 causes male and female infertility, and dramatically increase the number of p-bodies in *Drosophila* testis and eggs (Zabolotskaya et al. 2008, Lin et al. 2008). Also, overexpression of Ddx6 in neural stem cells (NSCs) leads to an increase in neuronal differentiation via activation of microRNA Let-7A (Nicklas et al. 2015). Therefore, Ddx6 is not directly related to obesity, but it is possible that overexpression of Ddx6 in *Xrn1-BKO* hypothalamus affects p-body formation or microRNA mediated gene silencing and causes inactivation of specific transcripts related to energy homeostasis in *Xrn1-BKO* hypothalamus.

In conclusion, I found that forebrain specific *Xrn1* knockout causes defects in energy homeostasis and leads to obesity and hyperphagia. In principle, *Xrn1* degrades bulk mRNAs, however, *Xrn1-BKO* mice exhibited very specific phenotype. Moreover, I found that dysregulated expression of appetite and energy homeostasis related genes in the hypothalamus of the knockout mice. This result suggests that either 5'-3' decay in the brain has the particular target mRNAs or, majority of 5'-3' decay targets are degraded by different decay pathways such as 3'-5' decay in *Xrn1-BKO* mice. Therefore, elucidation of the molecular mechanisms of obesity and energy homeostasis regulation by *Xrn1* would raise the possibility of developing therapeutic strategies to treat metabolic defects such as obesity and diabetes.

References

- Abernathy, Emma, Sarah Gilbertson, Ravi Alla, and Britt Glaunsinger. 2015. "Viral Nucleases Induce an mRNA Degradation-Transcription Feedback Loop in Mammalian Cells." *Cell host & microbe* 18 (2):243-253. doi: 10.1016/j.chom.2015.06.019.
- Agnès, François, Suzanne Magali, and Stéphane Noselli. 1999. "The Drosophila JNK pathway controls the morphogenesis of imaginal discs during metamorphosis." *Development (Cambridge, England)* 126 (23):5453-5462.
- Allmang, Christine, Elisabeth Petfalski, Alexandre Podtelejnikov, Matthias Mann, David Tollervey, and Philip Mitchell. 1999. "The yeast exosome and human PM-Scl are related complexes of 3' → 5' exonucleases." *Genes & development* 13 (16):2148-2158.
- Audic, Yann, and Rebecca S. Hartley. 2004. "Post-transcriptional regulation in cancer." *Biology of the Cell*. doi: 10.1016/j.biocel.2004.05.002.
- Babbarwal, Vinod, Jianhua Fu, and Joseph C. Reese. 2014. "The Rpb4/7 module of RNA polymerase II is required for carbon catabolite repressor protein 4-negative on TATA (Ccr4-not) complex to promote elongation." *The Journal of biological chemistry* 289 (48):33125-33130. doi: 10.1074/jbc.C114.601088.
- Badarinarayana, Vasudeo, Yueh-Chin Chiang, and Clyde L Denis. 2000. "Functional interaction of CCR4-NOT proteins with TATAA-binding protein (TBP) and its associated factors in yeast." *Genetics* 155 (3):1045-1054.
- Balland, Eglantine, and Michael A. Cowley. 2015. "New insights in leptin resistance mechanisms in mice." *Frontiers in neuroendocrinology* 39:59-65. doi: 10.1016/j.yfrne.2015.09.004.
- Barbee, Scott A, Patricia S Estes, Anne-Marie Cziko, Jens Hillebrand, Rene A Luedeman, Jeff M Collier, Nick Johnson, Iris C Howlett, Cuiyun Geng, Ryu Ueda, Andrea H Brand, Sarah F Newbury, James E Wilhelm, Richard B Levine, Akira Nakamura, Roy Parker, and Mani Ramaswami. 2006. "Staufen-and FMRP-containing neuronal RNPs are structurally and functionally related to somatic P bodies." *Neuron*.
- Bashkirov, VI., H. Scherthan, JA. Solinger, JM. Buerstedde, and WD. Heyer. 1997. "A mouse cytoplasmic exoribonuclease (mXRN1p) with preference for G4 tetraplex substrates." *The Journal of cell ...*
- Belgardt, Bengt F., Tomoo Okamura, and Jens C. Brüning. 2009. "Hormone and glucose signalling in POMC and AgRP neurons." *The Journal of physiology* 587 (Pt 22):5305-5314. doi: 10.1113/jphysiol.2009.179192.
- Benson, John D., Mark Benson, Peter M. Howley, and Kevin Struhl. 1998. "Association of distinct yeast Not2 functional domains with components of Gcn5 histone acetylase and Ccr4 transcriptional regulatory complexes." *The EMBO Journal*:6714-6722. doi: 10.1093/emboj/17.22.6714.
- Berthet, Cyril, Anne-Marie Morera, Marie-Jeanne Asensio, Marie-Agnes Chauvin, Anne-Pierre Morel, Frederique Dijoud, Jean-Pierre Magaud, Philippe Durand, and Jean-Pierre

- Rouault. 2004. "CCR4-associated factor CAF1 is an essential factor for spermatogenesis." *Molecular and cellular biology* 24 (13):5808-5820. doi: 10.1128/MCB.24.13.5808-5820.2004.
- Bjørnbæk, Christian, Joel K. Elmquist, J. Daniel Frantz, Steven E. Shoelson, and Jeffrey S. Flier. 1998. "Identification of SOCS-3 as a Potential Mediator of Central Leptin Resistance." *Molecular Cell* 1 (4):619-625. doi: 10.1016/S1097-2765(00)80062-3.
- Borbolis, Fivos, Christina-Maria Flessa, Fani Roumelioti, George Diallinas, Dimitrios J. Stravopodis, and Popi Syntichaki. 2017. "Neuronal function of the mRNA decapping complex determines survival of *Caenorhabditis elegans* at high temperature through temporal regulation of heterochronic gene expression." *Open biology* 7 (3):160313. doi: 10.1098/rsob.160313.
- Braun, J. E., V. Truffault, A. Boland, and E. Huntzinger. 2012. "A direct interaction between DCP1 and XRN1 couples mRNA decapping to 5' exonucleolytic degradation." *Nature structural & ...* doi: 10.1038/nsmb.2413.
- Braun, Katherine A., Stefania Vaga, Kenneth M. Dombek, Fang Fang, Salvator Palmisano, Ruedi Aebersold, and Elton T. Young. 2014. "Phosphoproteomic analysis identifies proteins involved in transcription-coupled mRNA decay as targets of Snf1 signaling." *Sci. Signal.* 7 (333). doi: 10.1126/scisignal.2005000.
- Braun, Katherine A., and Elton T. Young. 2014. "Coupling mRNA synthesis and decay." *Molecular and cellular biology* 34 (22):4078-4087. doi: 10.1128/MCB.00535-14.
- Buchan, Ross J., and Roy Parker. 2009. "Eukaryotic Stress Granules: The Ins and Outs of Translation." *Molecular Cell* 36 (6):932-941. doi: 10.1016/j.molcel.2009.11.020.
- Cavalcanti-de-Albuquerque, João, Jeremy Bober, Marcelo R. Zimmer, and Marcelo O. Dietrich. 2019. "Regulation of substrate utilization and adiposity by Agrp neurons." *Nature Communications* 10 (1):311. doi: 10.1038/s41467-018-08239-x.
- Chang, C. T., N. Bercovich, B. Loh, and S. Jonas. 2014. "The activation of the decapping enzyme DCP2 by DCP1 occurs on the EDC4 scaffold and involves a conserved loop in DCP1." *Nucleic acids ...* doi: 10.1093/nar/gku129.
- Chen, Chyi-Ying A., and Ann-Bin Shyu. 2011. "Mechanisms of deadenylation-dependent decay." *Wiley Interdisciplinary Reviews: RNA* 2 (2):167-183. doi: 10.1002/wrna.40.
- Chen, H., O. Charlat, L. A. Tartaglia, E. A. Wolf, X. Weng, S. J. Ellis, N. D. Lakey, J. Culpepper, K. J. Moore, R. E. Breitbart, G. M. Duyk, R. I. Tepper, and J. P. Morgenstern. 1996. "Evidence that the diabetes gene encodes the leptin receptor: identification of a mutation in the leptin receptor gene in db/db mice." *Cell* 84 (3):491-495. doi: 10.1016/S0092-8674(00)81294-5.
- Cheung, Alan C. M., and Patrick Cramer. 2011. "Structural basis of RNA polymerase II backtracking, arrest and reactivation." *Nature* 471 (7337):249-253. doi: 10.1038/nature09785.
- Choder, Mordechai. 2004. "Rpb4 and Rpb7: subunits of RNA polymerase II and beyond." *Trends in biochemical sciences* 29 (12):674-681. doi: 10.1016/j.tibs.2004.10.007.
- Coleman, D. L., and K. P. Hummel. 1967. "Studies with the mutation, diabetes, in the mouse."

- Diabetologia* 3 (2):238-248. doi: 10.1007/BF01222201.
- Coleman, D. L., and K. P. Hummel. 1973. "The influence of genetic background on the expression of the obese (ob) gene in the mouse." *Diabetologia*.
- Collart, Martine A. 2016. "The Ccr4-Not complex is a key regulator of eukaryotic gene expression." *Wiley interdisciplinary reviews. RNA*. doi: 10.1002/wrna.1332.
- Collart, Martine A., and Joseph C. Reese. 2014. "Gene expression as a circular process: Cross-talk between transcription and mRNA degradation in eukaryotes; International University of Andalusia (UNIA) Baeza, Spain." *RNA biology* 11 (4):320-323. doi: 10.4161/rna.28037.
- Coller, J. M., M. Tucker, U. Sheth, M. A. Valencia-Sanchez, and R. Parker. 2001. "The DEAD box helicase, Dhh1p, functions in mRNA decapping and interacts with both the decapping and deadenylase complexes." *RNA* 7 (12):1717-27. doi: 10.1017/s135583820101994x.
- Cougot, Nicolas, Sylvie Babajko, and Bertrand Séraphin. 2004. "Cytoplasmic foci are sites of mRNA decay in human cells." *The Journal of cell biology* 165 (1):31-40. doi: 10.1083/jcb.200309008.
- Cowley, M. A., J. L. Smart, M. Rubinstein, and Cerdán - M. G. Nature. 2001. "Leptin activates anorexigenic POMC neurons through a neural network in the arcuate nucleus." *Nature*. doi: 10.1038/35078085.
- Dubuc, P. U. 1976. "The development of obesity, hyperinsulinemia, and hyperglycemia in ob/ob mice." *Metabolism: clinical and experimental* 25 (12):1567-1574. doi: 10.1016/0026-0495(76)90109-8.
- Dutta, Arnob, Vinod Babbarwal, Jianhua Fu, Deborah Brunke-Reese, Diane M. Libert, Jonathan Willis, and Joseph C. Reese. 2015. "Ccr4-Not and TFIIS Function Cooperatively To Rescue Arrested RNA Polymerase II." *Molecular and cellular biology* 35 (11):1915-1925. doi: 10.1128/MCB.00044-15.
- Dziembowski, Andrzej, Esben Lorentzen, Elena Conti, and Bertrand Séraphin. 2007. "A single subunit, Dis3, is essentially responsible for yeast exosome core activity." *Nature structural & molecular biology* 14 (1):15-22. doi: 10.1038/nsmb1184.
- Farooqi, I. S., J. M. Keogh, G. S. H. Yeo, E. J. Lank, T. Cheetham, and S. O'Rahilly. 2003. "Clinical spectrum of obesity and mutations in the melanocortin 4 receptor gene." *... England Journal of* doi: 10.1056/NEJMoa022050.
- Fischer, N., and K. Weis. 2002. "The DEAD box protein Dhh1 stimulates the decapping enzyme Dcp1." *The EMBO journal*.
- Garneau, N. L., J. Wilusz, and C. J. Wilusz. 2007. "The highways and byways of mRNA decay." *Nature reviews Molecular cell* doi: 10.1038/nrm2104.
- Graham, M., J. R. Shutter, U. Sarmiento, I. Sarosi, and K. L. Stark. 1997. "Overexpression of Agrt leads to obesity in transgenic mice." *Nature genetics* 17 (3):273-274. doi: 10.1038/ng1197-273.
- Grima, DP., M. Sullivan, MV. Zabolotskaya, C. Browne, J. Seago, Wan KC, Y. Okada, and SF. Newbury. 2008. "The 5'-3' exoribonuclease pacman is required for epithelial

- sheet sealing in *Drosophila* and genetically interacts with the phosphatase puckered." *Biology of the ...* doi: 10.1042/BC20080049.
- Haimovich, Gal, Daniel A. Medina, Sebastien Z. Causse, Manuel Garber, Gonzalo Millán-Zambrano, Oren Barkai, Sebastián Chávez, José E. E. Pérez-Ortín, Xavier Darzacq, and Mordechai Choder. 2013. "Gene expression is circular: factors for mRNA degradation also foster mRNA synthesis." *Cell* 153 (5). doi: 10.1016/j.cell.2013.05.012.
- Haruki, H., J. Nishikawa, and U. K. Laemmli. 2008. "The anchor-away technique: rapid, conditional establishment of yeast mutant phenotypes." *Molecular cell*. doi: 10.1016/j.molcel.2008.07.020.
- Horvath, Tamas L., Ingo Bechmann, Frederick Naftolin, Satya P. Kalra, and Csaba Leranth. 1997. "Heterogeneity in the neuropeptide Y-containing neurons of the rat arcuate nucleus: GABAergic and non-GABAergic subpopulations." *Brain Research* 756 (1-2):283-286. doi: 10.1016/S0006-8993(97)00184-4.
- Hu, Fang, Yong Xu, and Feng Liu. 2016. "Hypothalamic roles of mTOR complex I: integration of nutrient and hormone signals to regulate energy homeostasis." *American journal of physiology. Endocrinology and metabolism* 310 (11). doi: 10.1152/ajpendo.00121.2016.
- Huang, Xingjun, Guihua Liu, Jiao Guo, and Zhengquan Su. 2018. "The PI3K/AKT pathway in obesity and type 2 diabetes." *International Journal of Biological Sciences* 14 (11):1483-1496. doi: 10.7150/ijbs.27173.
- Huszar, D., C. A. Lynch, V. Fairchild-Huntress, J. H. Dunmore, Q. Fang, L. R. Berkemeier, W. Gu, R. A. Kesterson, B. A. Boston, R. D. Cone, F. J. Smith, L. A. Campfield, P. Burn, and F. Lee. 1997. "Targeted disruption of the melanocortin-4 receptor results in obesity in mice." *Cell* 88 (1):131-141. doi: 10.1016/S0092-8674(00)81865-6.
- Ingalls, Ann M., Margaret M. Dickie, and G. D. Snell. 1950. "OBESE, A NEW MUTATION IN THE HOUSE MOUSE*." *Journal of Heredity* 41 (12):317-318. doi: 10.1093/oxfordjournals.jhered.a106073.
- Inoue, Takeshi, Masahiro Morita, Atsushi Hijikata, Yoko Fukuda-Yuzawa, Shungo Adachi, Kyoichi Isono, Tomokatsu Ikawa, Hiroshi Kawamoto, Haruhiko Koseki, Tohru Natsume, Taro Fukao, Osamu Ohara, Tadashi Yamamoto, and Tomohiro Kurosaki. 2015. "CNOT3 contributes to early B cell development by controlling Igh rearrangement and p53 mRNA stabilityRegulation of early B cell development by CNOT3." *The Journal of Experimental Medicine* 212 (9):1465-1479. doi: 10.1084/jem.20150384.
- Ito, Kentaro, Takeshi Inoue, Kazumasa Yokoyama, Masahiro Morita, Toru Suzuki, and Tadashi Yamamoto. 2011. "CNOT2 depletion disrupts and inhibits the CCR4-NOT deadenylase complex and induces apoptotic cell death." *Genes to cells : devoted to molecular & cellular mechanisms* 16 (4):368-379. doi: 10.1111/j.1365-2443.2011.01492.x.
- Ito, Kentaro, Akinori Takahashi, Masahiro Morita, Toru Suzuki, and Tadashi Yamamoto. 2011. "The role of the CNOT1 subunit of the CCR4-NOT complex in mRNA deadenylation and cell viability." *Protein & cell* 2 (9):755-763. doi: 10.1007/s13238-011-1092-4.
- Jacinto, A., A. Martinez-Arias, and P. Martin. 2001. "Mechanisms of epithelial fusion and repair." *Nature cell biology* 3 (5):23. doi: 10.1038/35074643.

- Jacinto, Antonio, Sarah Woolner, and Paul Martin. 2002. "Dynamic analysis of dorsal closure in *Drosophila*: from genetics to cell biology." *Developmental cell* 3 (1):9-19. doi: 10.1016/s1534-5807(02)00208-3.
- James, Nicole, Emilie Landrieux, and Martine A. Collart. 2007. "A SAGA-independent function of SPT3 mediates transcriptional deregulation in a mutant of the Ccr4-not complex in *Saccharomyces cerevisiae*." *Genetics* 177 (1):123-135. doi: 10.1534/genetics.107.076299.
- Jayne, Sandrine, Carin G. Zwartjes, Frederik M. van Schaik, and H. T. Timmers. 2006. "Involvement of the SMRT/NCOR-HDAC3 complex in transcriptional repression by the CNOT2 subunit of the human Ccr4-Not complex." *The Biochemical journal* 398 (3):461-467. doi: 10.1042/BJ20060406.
- Jones, Christopher I., Maria V. Zabolotskaya, and Sarah F. Newbury. 2012. "The 5' → 3' exoribonuclease XRN1/Pacman and its functions in cellular processes and development." *Wiley interdisciplinary reviews. RNA* 3 (4):455-468. doi: 10.1002/wrna.1109.
- Kanasaki, Keizo, and Daisuke Koya. 2011. "Biology of obesity: lessons from animal models of obesity." *Journal of biomedicine & biotechnology* 2011:197636. doi: 10.1155/2011/197636.
- Kiebler, Michael A., and Gary J. Bassell. 2006. "Neuronal RNA Granules: Movers and Makers." *Neuron* 51 (6):685-690. doi: 10.1016/j.neuron.2006.08.021.
- Koutelou, Evangelia, Calley L. Hirsch, and Sharon Y. R. Dent. 2010. "Multiple faces of the SAGA complex." *Current Opinion in Cell Biology*:374-382. doi: 10.1016/j.ceb.2010.03.005.
- Kruk, Jennifer A., Arnob Dutta, Jianhua Fu, David S. Gilmour, and Joseph C. Reese. 2011. "The multifunctional Ccr4-Not complex directly promotes transcription elongation." *Genes & Development* 25 (6):581-593. doi: 10.1101/gad.2020911.
- LaGrandeur, Thomas E., and Roy Parker. 1998. "Isolation and characterization of Dcp1p, the yeast mRNA decapping enzyme." *The EMBO Journal* 17 (5):1487-1496. doi: 10.1093/emboj/17.5.1487.
- Larimer, F. W., and A. Stevens. 1990. "Disruption of the gene XRN1, coding for a 5'----3' exoribonuclease, restricts yeast cell growth." *Gene* 95 (1):85-90. doi: 10.1016/0378-1119(90)90417-p.
- Lin, Ming-Der, Xinfu Jiao, Dominic Grima, Sarah F. Newbury, Megerditch Kiledjian, and Tze-Bin Chou. 2008. "Drosophila processing bodies in oogenesis." *Developmental biology* 322 (2):276-288. doi: 10.1016/j.ydbio.2008.07.033.
- Linder, Bastian, Utz Fischer, and Niels H. Gehring. 2015. "mRNA metabolism and neuronal disease." *FEBS letters*. doi: 10.1016/j.febslet.2015.04.052.
- Liu, Hudan, Nancy D. Rodgers, Xinfu Jiao, and Megerditch Kiledjian. 2002. "The scavenger mRNA decapping enzyme DcpS is a member of the HIT family of pyrophosphatases." *The EMBO journal* 21 (17):4699-4708. doi: 10.1093/emboj/cdf448.
- Loh, Kim, Atsushi Fukushima, Xinmei Zhang, Sandra Galic, Dana Briggs, Pablo J. Enriori,

- Stephanie Simonds, Florian Wiede, Alexander Reichenbach, Christine Hauser, Natalie A. Sims, Kendra K. Bence, Sheng Zhang, Zhong-Yin Y. Zhang, Barbara B. Kahn, Benjamin G. Neel, Zane B. Andrews, Michael A. Cowley, and Tony Tiganis. 2011. "Elevated hypothalamic TCPTP in obesity contributes to cellular leptin resistance." *Cell metabolism* 14 (5):684-699. doi: 10.1016/j.cmet.2011.09.011.
- Lotan, Rona, Vicky G. Bar-On, Liat Harel-Sharvit, Lea Duek, Daniel Melamed, and Mordechai Choder. 2005. "The RNA polymerase II subunit Rpb4p mediates decay of a specific class of mRNAs." *Genes & development* 19 (24):3004-3016. doi: 10.1101/gad.353205.
- Luchelli, Luciana, María G. G. Thomas, and Graciela L. Boccaccio. 2015. "Synaptic control of mRNA translation by reversible assembly of XRN1 bodies." *Journal of cell science* 128 (8):1542-1554. doi: 10.1242/jcs.163295.
- Mang, Géraldine M., Sylvain Pradervand, Ngoc-Hien Du, Alaaddin Arpat, Frédéric Preitner, Leonore Wigger, David Gatfield, and Paul Franken. 2015. "A Neuron-Specific Deletion of the MicroRNA-Processing Enzyme DICER Induces Severe but Transient Obesity in Mice." *PLOS ONE* 10 (1). doi: 10.1371/journal.pone.0116760.
- Morita, Masahiro, Yuichi Oike, Takeshi Nagashima, Tsuyoshi Kadomatsu, Mitsuhisa Tabata, Toru Suzuki, Takahisa Nakamura, Nobuaki Yoshida, Mariko Okada, and Tadashi Yamamoto. 2011. "Obesity resistance and increased hepatic expression of catabolism-related mRNAs in Cnot3^{+/-} mice." *The EMBO journal* 30 (22):4678-4691. doi: 10.1038/emboj.2011.320.
- Morita, Masahiro, Nadeem Siddiqui, Sakie Katsumura, Christopher Rouya, Ola Larsson, Takeshi Nagashima, Bahareh Hekmatnejad, Akinori Takahashi, Hiroshi Kiyonari, Mengwei Zang, René St-Arnaud, Yuichi Oike, Vincent Giguère, Ivan Topisirovic, Mariko Okada-Hatakeyama, Tadashi Yamamoto, and Nahum Sonenberg. 2019. "Hepatic posttranscriptional network comprised of CCR4-NOT deadenylase and FGF21 maintains systemic metabolic homeostasis." *Proceedings of the National Academy of Sciences of the United States of America* 116 (16):7973-7981. doi: 10.1073/pnas.1816023116.
- Moser, M. J., W. R. Holley, A. Chatterjee, and I. S. Mian. 1997. "The proofreading domain of Escherichia coli DNA polymerase I and other DNA and/or RNA exonuclease domains." *Nucleic acids research* 25 (24):5110-5118.
- Nakamura, Takahisa, Ryoji Yao, Takehiko Ogawa, Toru Suzuki, Chizuru Ito, Naoki Tsunekawa, Kimiko Inoue, Rieko Ajima, Takashi Miyasaka, Yutaka Yoshida, Atsuo Ogura, Kiyotaka Toshimori, Toshiaki Noce, Tadashi Yamamoto, and Tetsuo Noda. 2004. "Oligo-asthenoteratozoospermia in mice lacking Cnot7, a regulator of retinoid X receptor beta." *Nature genetics* 36 (5):528-533. doi: 10.1038/ng1344.
- Newbury, Sarah, and Alison Woollard. 2004. "The 5'-3' exoribonuclease xrn-1 is essential for ventral epithelial enclosure during C. elegans embryogenesis." *RNA* 10 (1):59-65. doi: 10.1261/rna.2195504.
- Nicklas, S., S. Okawa, AL. Hillje, L. González-Cano, A. Del Sol, and JC. Schwamborn. 2015.

- "The RNA helicase DDX6 regulates cell-fate specification in neural stem cells via miRNAs." *Nucleic acids ...* doi: 10.1093/nar/gkv138.
- Ollmann, Michael M., Brent D. Wilson, Ying-Kui Yang, Julie A. Kerns, Yanru Chen, Ira Gantz, and Gregory S. Barsh. 1997. "Antagonism of Central Melanocortin Receptors in Vitro and in Vivo by Agouti-Related Protein." *Science* 278 (5335):135-138. doi: 10.1126/science.278.5335.135.
- Olofsson, Louise E., Elizabeth K. Unger, Clement C. Cheung, and Allison W. Xu. 2013. "Modulation of AgRP-neuronal function by SOCS3 as an initiating event in diet-induced hypothalamic leptin resistance." *Proceedings of the National Academy of Sciences* 110 (8). doi: 10.1073/pnas.1218284110.
- Parker, R., and U. Sheth. 2007. "P bodies and the control of mRNA translation and degradation." *Molecular cell*.
- Parker, Roy, and Haiwei Song. 2004. "The enzymes and control of eukaryotic mRNA turnover." *Nature structural & molecular biology* 11 (2):121-127. doi: 10.1038/nsmb724.
- Pritchard, L. E., A. V. Turnbull, and A. White. 2002. "Pro-opiomelanocortin processing in the hypothalamus: impact on melanocortin signalling and obesity." *Journal of Endocrinology* 172 (3):411-421. doi: 10.1677/joe.0.1720411.
- Radhakrishnan, A. , and R. Green. 2016. "Connections underlying translation and mRNA stability." *Journal of molecular biology*.
- Reed, Alison S., Elizabeth K. Unger, Louise E. Olofsson, Merisa L. Piper, Martin G. Myers, and Allison W. Xu. 2010. "Functional Role of Suppressor of Cytokine Signaling 3 Upregulation in Hypothalamic Leptin Resistance and Long-Term Energy Homeostasis." *Diabetes* 59 (4):894-906. doi: 10.2337/db09-1024.
- Rousakis, Aris, Anna Vlantzi, Fivos Borbolis, Fani Roumelioti, Marianna Kapetanou, and Popi Syntichaki. 2014. "Diverse functions of mRNA metabolism factors in stress defense and aging of *Caenorhabditis elegans*." *PloS one* 9 (7). doi: 10.1371/journal.pone.0103365.
- Russell, Pamela, John D. Benson, and Clyde L. Denis. 2002. "Characterization of mutations in NOT2 indicates that it plays an important role in maintaining the integrity of the CCR4-NOT complex." *Journal of molecular biology* 322 (1):27-39.
- Sabapathy, Kanaga, Wolfram Jochum, Konrad Hochedlinger, Lufen Chang, Michael Karin, and Erwin F. Wagner. 1999. "Defective neural tube morphogenesis and altered apoptosis in the absence of both JNK1 and JNK2." *Mechanisms of Development* 89 (1-2):115-124. doi: 10.1016/S0925-4773(99)00213-0.
- Salem, Esam S. B., Andrew D. Vonberg, Vishnupriya J. Borra, Rupinder K. Gill, and Takahisa Nakamura. 2019. "RNAs and RNA-Binding Proteins in Immuno-Metabolic Homeostasis and Diseases." *Frontiers in Cardiovascular Medicine* 6:106. doi: 10.3389/fcvm.2019.00106.
- She, Meipei, Carolyn J. Decker, Dmitri I. Svergun, Adam Round, Nan Chen, Denise Muhrad, Roy Parker, and Haiwei Song. 2008. "Structural basis of dcp2 recognition and activation by dcp1." *Molecular cell* 29 (3):337-349. doi: 10.1016/j.molcel.2008.01.002.
- Sheth, Ujwal, and Roy Parker. 2003. "Decapping and decay of messenger RNA occur in

- cytoplasmic processing bodies." *Science (New York, N.Y.)* 300 (5620):805-808. doi: 10.1126/science.1082320.
- Shirai, Yo-Taro., Toru Suzuki, Masahiro Morita, Akinori Takahashi, and Tadashi Yamamoto. 2014. "Multifunctional roles of the mammalian CCR4-NOT complex in physiological phenomena." *Frontiers in genetics* 5:286. doi: 10.3389/fgene.2014.00286.
- Song, M. G., Y. Li, and M. Kiledjian. 2010. "Multiple mRNA decapping enzymes in mammalian cells." *Molecular cell*.
- St-Pierre, Julie, and Michel L. Tremblay. 2012. "Modulation of leptin resistance by protein tyrosine phosphatases." *Cell metabolism* 15 (3):292-297. doi: 10.1016/j.cmet.2012.02.004.
- Steiger, Michelle, Anne Carr-Schmid, David C. Schwartz, Megerditch Kiledjian, and Roy Parker. 2003. "Analysis of recombinant yeast decapping enzyme." *RNA (New York, N.Y.)* 9 (2):231-238. doi: 10.1261/rna.2151403.
- Sun, Mai, Björn Schwalb, Nicole Pirkl, Kerstin C. Maier, Arne Schenk, Henrik Failmezger, Achim Tresch, and Patrick Cramer. 2013. "Global analysis of eukaryotic mRNA degradation reveals Xrn1-dependent buffering of transcript levels." *Molecular cell* 52 (1):52-62. doi: 10.1016/j.molcel.2013.09.010.
- Sun, Mai, Björn Schwalb, Daniel Schulz, Nicole Pirkl, Stefanie Etzold, Laurent Larivière, Kerstin C. Maier, Martin Seizl, Achim Tresch, and Patrick Cramer. 2012. "Comparative dynamic transcriptome analysis (cDTA) reveals mutual feedback between mRNA synthesis and degradation." *Genome research* 22 (7). doi: 10.1101/gr.130161.111.
- Suzuki, Toru, Chisato Kikuguchi, Saori Nishijima, Takeshi Nagashima, Akinori Takahashi, Mariko Okada, and Tadashi Yamamoto. 2019. "Postnatal liver functional maturation requires Cnot complex-mediated decay of mRNAs encoding cell cycle and immature liver genes." *Development (Cambridge, England)* 146 (4). doi: 10.1242/dev.168146.
- Suzuki, Toru, Chisato Kikuguchi, Sahil Sharma, Toshio Sasaki, Miho Tokumasu, Shungo Adachi, Tohru Natsume, Yumi Kanegae, and Tadashi Yamamoto. 2015. "CNOT3 suppression promotes necroptosis by stabilizing mRNAs for cell death-inducing proteins." *Scientific reports* 5:14779. doi: 10.1038/srep14779.
- Takahashi, Akinori, Shungo Adachi, Masahiro Morita, Miho Tokumasu, Tohru Natsume, Toru Suzuki, and Tadashi Yamamoto. 2015. "Post-transcriptional Stabilization of Ucp1 mRNA Protects Mice from Diet-Induced Obesity." *Cell reports* 13 (12):2756-2767. doi: 10.1016/j.celrep.2015.11.056.
- Takahashi, Akinori, Shohei Takaoka, Shungo Kobori, Tomokazu Yamaguchi, Sara Ferwati, Keiji Kuba, Tadashi Yamamoto, and Toru Suzuki. 2019. "The CCR4-NOT Deadenylase Complex Maintains Adipocyte Identity." *International Journal of Molecular Sciences* 20 (21):5274. doi: 10.3390/ijms20215274.
- Tanti, Jean-François, Franck Ceppo, Jennifer Jager, Flavien Berthou, Jean-François Tanti, Franck Ceppo, Jennifer Jager, and Flavien Berthou. 2013. "Implication of inflammatory signaling pathways in obesity-induced insulin resistance." *Frontiers in Endocrinology*. doi: 10.3389/fendo.2012.00181.

- Thomas, María G. G., and Graciela L. Boccaccio. 2016. "Novel mRNA-silencing bodies at the synapse: A never-ending story." *Communicative & integrative biology* 9 (2). doi: 10.1080/19420889.2016.1139251.
- Thomas, MG. , LJ. Martinez Tosar, MA. Desbats, CC. Leishman, and GL. Boccaccio. 2009. "Mammalian Staufen 1 is recruited to stress granules and impairs their assembly." *Journal of cell* doi: 10.1242/jcs.038208.
- Tong, Qingchun, Chian-Ping Ye, Juli E. Jones, Joel K. Elmquist, and Bradford B. Lowell. 2008. "Synaptic release of GABA by AgRP neurons is required for normal regulation of energy balance." *Nature neuroscience* 11 (9):998-1000. doi: 10.1038/nn.2167.
- Vyas, Valmik K., Cristin D. Berkey, Takenori Miyao, and Marian Carlson. 2005. "Repressors Nrg1 and Nrg2 regulate a set of stress-responsive genes in *Saccharomyces cerevisiae*." *Eukaryotic cell* 4 (11):1882-1891. doi: 10.1128/EC.4.11.1882-1891.2005.
- Watanabe, Chiho, Masahiro Morita, Tadayoshi Hayata, Tetsuya Nakamoto, Chisato Kikuguchi, Xue Li, Yasuhiro Kobayashi, Naoyuki Takahashi, Takuya Notomi, Keiji Moriyama, Tadashi Yamamoto, Yoichi Ezura, and Masaki Noda. 2014. "Stability of mRNA influences osteoporotic bone mass via CNOT3." *Proceedings of the National Academy of Sciences of the United States of America* 111 (7):2692-2697. doi: 10.1073/pnas.1316932111.
- White, Christy L., Amy Whittington, Maria J. Barnes, Zhong Wang, George A. Bray, and Christopher D. Morrison. 2009. "HF diets increase hypothalamic PTP1B and induce leptin resistance through both leptin-dependent and -independent mechanisms." *American Journal of Physiology-Endocrinology and Metabolism* 296 (2). doi: 10.1152/ajpendo.90513.2008.
- Wojtas, Magdalena N., Radha R. Pandey, Mateusz Mendel, David Homolka, Ravi Sachidanandam, and Ramesh S. Pillai. 2017. "Regulation of m(6)A Transcripts by the 3'→5' RNA Helicase YTHDC2 Is Essential for a Successful Meiotic Program in the Mammalian Germline." *Molecular cell* 68 (2):374-1971793920. doi: 10.1016/j.molcel.2017.09.021.
- Wunderlich, Claudia M., Nadine Hövelmeyer, and Thomas F. Wunderlich. 2013. "Mechanisms of chronic JAK-STAT3-SOCS3 signaling in obesity." *JAK-STAT* 2 (2). doi: 10.4161/jkst.23878.
- Yamaguchi, Tomokazu, Takashi Suzuki, Teruki Sato, Akinori Takahashi, Hiroyuki Watanabe, Ayumi Kadowaki, Miyuki Natsui, Hideaki Inagaki, Satoko Arakawa, Shinji Nakaoka, Yukio Koizumi, Shinsuke Seki, Shungo Adachi, Akira Fukao, Toshinobu Fujiwara, Tohru Natsume, Akinori Kimura, Masaaki Komatsu, Shigeomi Shimizu, Hiroshi Ito, Yutaka Suzuki, Josef M. Penninger, Tadashi Yamamoto, Yumiko Imai, and Keiji Kuba. 2018. "The CCR4-NOT deadenylase complex controls Atg7-dependent cell death and heart function." *Science Signaling* 11 (516). doi: 10.1126/scisignal.aan3638.
- Yamashita, Akio, Tsung-Cheng Chang, Yukiko Yamashita, Wenmiao Zhu, Zhenping Zhong, Chyi-Ying A. Chen, and Ann-Bin Shyu. 2005. "Concerted action of poly(A) nucleases and decapping enzyme in mammalian mRNA turnover." *Nature Structural &*

- Molecular Biology* 12 (12):1054-1063. doi: 10.1038/nsmb1016.
- Yaswen, L., N. Diehl, M. B. Brennan, and U. Hochgeschwender. 1999. "Obesity in the mouse model of pro-opiomelanocortin deficiency responds to peripheral melanocortin." *Nature medicine* 5 (9):1066-1070. doi: 10.1038/12506.
- Yazdi, Fereshteh T., Susanne M. Clee, and David Meyre. 2015. "Obesity genetics in mouse and human: back and forth, and back again." *PeerJ* 3. doi: 10.7717/peerj.856.
- Zabolotskaya, Maria V., Dominic P. Grima, Ming-Der D. Lin, Tze-Bin B. Chou, and Sarah F. Newbury. 2008. "The 5'-3' exoribonuclease Pacman is required for normal male fertility and is dynamically localized in cytoplasmic particles in *Drosophila* testis cells." *The Biochemical journal* 416 (3):327-335. doi: 10.1042/BJ20071720.
- Zhang, Xiaoqing, Guo Zhang, Hai Zhang, Michael Karin, Hua Bai, and Dongsheng Cai. 2008. "Hypothalamic IKK β /NF- κ B and ER Stress Link Overnutrition to Energy Imbalance and Obesity." *Cell* 135 (1):61-73. doi: 10.1016/j.cell.2008.07.043.
- Zhang, Yiying, Ricardo Proenca, Margherita Maffei, Marisa Barone, Lori Leopold, and Jeffrey M. Friedman. 1994. "Positional cloning of the mouse obese gene and its human homologue." *Nature* 372 (6505):425-432. doi: 10.1038/372425a0.
- Zwartjes, Carin G., Sandrine Jayne, Debbie L. van den Berg, and H. T. Timmers. 2004. "Repression of promoter activity by CNOT2, a subunit of the transcription regulatory Ccr4-not complex." *The Journal of biological chemistry* 279 (12):10848-10854. doi: 10.1074/jbc.M311747200.